Aerogels and Related Porous Materials

H. D. GESSER* and P. C. GOSWAMI

Department of Chemistry, University of Manitoba, Winnipeg, Manitoba, Canada R3T 2N2, and spdf Chemical Association Ltd., Winnipeg, Manitoba, Canada R3T 2N2

Contents

Overview

Aerogels are extremely porous, low-density materials, consisting of inorganic oxides such as silica, alumina, zirconia, stannic or tungsten oxide, or a mixture of these oxides. They have large surface areas and can be translucent as well as transparent, have extremely low thermal conductivities, and have fascinating acoustic properties (sound velocities as low as 100 m/s). This review surveys the literature and summarizes the historical background of aerogel development, their production by the sol–gel process, possible drying methods, structural investigations, and various novel applications in catalysis, high-energy physics, passive solar energy uses and energy conversions, and low-temperature glass formation.

I. Introduction

Aerogels are coherent, porous solids made by the formation of a colloidal gel followed by removal of the liquid from within the pores of the gel. They are usually of very low density, can be made in large pieces (monolithic structure), and can also be transparent. Aerogels

Hyman D. Gesser received his Ph.D. degree from McGill University. Following Postdoctoral Fellowships at the University of Rochester and N.R.C.—Ottawa, he joined the University of Manitoba in 1955. He is presently a Professor in the Chemistry Department. His current research interests are in high-pressure partial oxidation reactions, surface free radical reactions, photochemistry, and catalysis.

Prabhat C. Goswami received his B.Sc. (Honors) and M.Sc. degrees in chemistry from the Gauhati University in Assam, India. He did graduate studies in physical chemistry at Bryn Mawr College, where he obtained his Ph.D. in 1970. He taught at the University of Ghana and at the University of Garyounis in Benghazi, Libya. His research interests are in photochemistry and spectroscopy. Since 1984, he has been a Research Associate in the Department of Chemistry, University of Manitoba, involved in research in overtone spectroscopy, production of aerogels, and free radical reactions on porous glasses.

had little practical value until 1974, when Cantin et al.[1] reported on the use of silica aerogels as detectors in Cerenkov radiation. More recently, they have found application as insulation in dual-pane windows (Super Windows),[2] and this has resulted in renewed interest in their production and optimization. Recent reviews on the subject have appeared.[3] Teichner and his group

compiled a review in 1976[4] and Schmitt, in his M.Sc. Thesis on the preparation of silica aerogels, presented an excellent review in 1982.[5] A review of transition-metal oxide gels and colloids was presented in 1982 by Livage and Lemerle.[6] The First International Symposium on Aerogels was held Sept 23–25, 1985, at Wurzburg, West Germany, and the papers presented there covering all aspects of the preparation, properties, and applications have been published.[7]

This review is concerned primarily with literature (both published and patented) on the preparation, structural aspects, and applications of monolithic coherent inorganic aerogels and related porous materials.

A. Definition of Terms

We begin with definitions of a few terms used throughout this review.

Sol: The term refers to a colloidal system of liquid character in which the dispersed particles are either solid or large molecules whose dimensions are in the colloidal range (1–1000 nm).

Gel: A gel is a colloidal system of solid character in which the dispersed substance forms a continuous, ramifying, coherent framework that is interpenetrated by a system (usually liquid) consisting of kinetic units smaller than colloidal entities. Gels frequently contain only a small amount of the dispersed phase (1–3%) and exhibit some measure of rigidity and elasticity, the rigidity being associated with the interaction between particles that are linked together in some manner. The assembly of primary units may be held together at the junction points by primary valence bonds, hydrogen bonds, dipole forces, van der Waals forces, or even mechanical entanglement.

The gels are usually classified according to the dispersion medium used, e.g., hydrogel or aquagel, alcogel, and aerogel (for water, alcohol, and air, respectively).

Xerogel: If the liquid within the gel is removed by simple evaporation, the formation of a liquid–vapor interface within the gel results in surface tension creating concave menisci in the pores of the gel. With the progress of evaporation, the menisci recede into the gel body and the buildup of compressive force acting on the walls of the pores causes considerable shrinkage due to partial collapse of the gel network. The collapse ceases when the gel structure is strong enough to withstand the tensile strength of the liquid, and the resultant hardened glassy, but still porous masses, are called xerogels. To avoid cracking or fragmentation, slow drying is usually essential.

Aerogels: Aerogels are obtained when the liquid within the gel is removed above its critical temperature and pressure (i.e., under supercritical or hypercritical conditions). This procedure is conducted in an autoclave so that the liquid in the gel is held under pressure always greater than its vapor pressure. As the pressure is raised, the liquid is transformed at its critical temperature into a fluid without liquid–vapor phases being present at any time. The fluid within the gel can be slowly extracted (so as not to injure the gel) at temperatures and pressure above the critical conditions to obtain an air-filled gel structure. Under supercritical conditions there is no distinction between liquid and vapor, no liquid–vapor meniscus, and therefore no surface tension or capillary pressure developed during

drying. The absence of surface tension allows the gel to be dried with very little shrinkage and the gel matrix to remain nearly intact. Such a gel consists of a dry network of solid containing large amounts of almost homogeneously dispersed air within the structure (e.g., for silica aerogel 5% silica, 95% fine pores). This microscopically fine dispersion of air in solid endows the material with many unusual properties more characteristic of a dense gas than a solid. Both xerogels and aerogels can be transparent or translucent solids but aerogels have higher surface areas, lower densities, larger pore sizes, and greater pore volumes.

Cryogel: Another way to avoid a liquid–vapor interface and hence pressure developing within the pores of the gel requires that the liquid first be frozen into a solid and then sublimed.[8] The vapor can be removed by vacuum pumping, and the resultant aerogel is called a cryogel[9] since cryogenic conditions are normally involved in drying.

B. Physics and Chemistry of Supercritical Fluid Drying

Drying an alcogel requires the removal of the interstitial liquid and its replacement with a dry gas. The method used to remove the liquid influences the characteristics of the dried gel.

During the drying process, liquid and vapor coexist within the pores of the gel. As the liquid begins to evaporate, at the liquid–vapor interface a meniscus is formed due to surface tension resulting from an imbalance of intermolecular attractions into the bulk of each phase. Since this surface energy is responsible for the rise of a column of liquid in a capillary, the magnitude of the interfacial pressure within a capillary can be calculated by balancing the static forces:[5]

$$2\sigma r \cos \theta = r^2 h \rho g \qquad (1)$$

or

$$\rho g h = P_s = \frac{2\sigma}{r} \cos \theta \qquad (2)$$

where θ is the contact angle between the liquid and the wall of the capillary. For ethanol on glass this is taken as 0°. For evaporation from a straight cylindrical pore of radius 20 nm filled with ethanol, $\sigma = 22.75$ dyn cm^{-1}; ρ (the density of ethanol) = 0.7893 g cm^{-3}, and P_s, the hydrostatic pressure equivalent to the surface force per unit area, is calculated to be 22.5 atm.

Since this force acts on a very small area where the wetted capillary wall and meniscus meet, the wall will not be able to withstand such a highly localized stress and will contract, eventually collapsing the gel body. In this process some bonds have to be broken to allow for the shrinkage. For a gel composed of small particles where the density is high, severe fragmentation may occur on drying but for a gelatinous and soft gel, a compact, porous crack-free dry mass (xerogel) can be obtained.

In practice, it is possible to eliminate the internal tensile forces in the pores of a gel by preventing the liquid–vapor boundary from developing. This is achieved by supercritical drying in an autoclave. The principles involved can be visualized with the *P–V–T* diagram (Figure 1) for ethanol. If the solvent in the pore is suddenly put under pressure greater than its
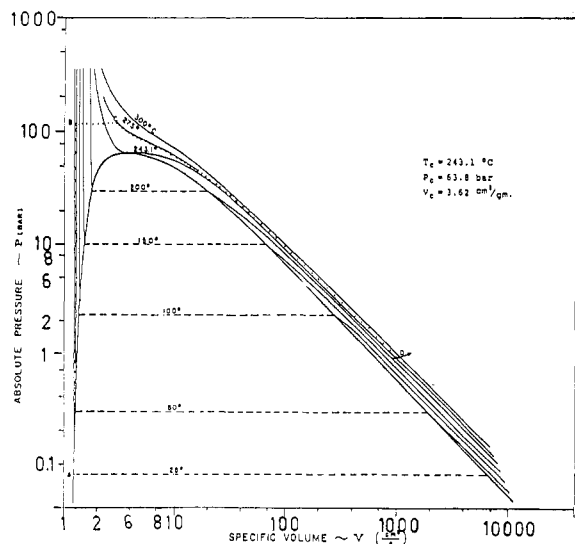
Figure 1. *P-V-T* diagram of ethanol. Reprinted with permission from ref 5; copyright 1982, University of Wisconsin, Madison.

critical pressure and then slowly heated isobarically (by releasing some solvent) to a temperature 20–25 °C above the critical temperature, the liquid will expand but not boil at such a high pressure. The system will remain as a single phase. At the critical point, the liquid ceases to be a liquid in the thermodynamic sense and is termed a fluid. Since two fluid phases are never formed with sufficient alcohol to keep the solid covered and still reach the critical pressure, no interfacial tension is created in the pores. The supercritical drying path is shown in the diagram (Figure 1) as ABCD. At point C, the temperature is held constant by adjusting the heat while ethanol is released at a rate so as not to injure the gel until ambient pressure, represented by D, is reached. A dry inert gas could be used at this stage to flush the autoclave to prevent ethanol from condensing onto the gel upon cooling. When ambient temperature is reached, a porous dried aerogel filled with air is obtained. Supercritical drying is a relatively faster technique than sublimation since mass transfer rates are high for the dense supercritical fluid.

Another variant of supercritical drying of alcogel involves liquid carbon dioxide. At 35 °C and 70 atm ethanol is a liquid but carbon dioxide is a fluid, and under these conditions they are miscible. It is possible to exchange ethanol with an excess of supercritical carbon dioxide in a continuous process. The ethanol-free gel can eventually be dried supercritically with respect to carbon dioxide at 35 °C.

II. Early Work

The first report on the preparation of coherent expanded aerogels was published by Kistler in 1931.[10] He clearly showed that the inorganic gel, when dehydrated under normal conditions, collapses into a powder as a result of the disruption in the pore structure of the gel. However, when the gel was dehydrated under supercritical conditions of temperature and pressure, the liquid–vapor boundary within the pores of the gel no longer existed and the gels did not collapse on drying. Kistler described the formation of gels of silica, alumina, ferric oxide, stannic oxide, tungstic oxide, nickel oxide, and several organic materials. Silica gels were made by hydrolyzing water glass with hydrochloric acid and

allowing the gel to set. It was then washed until the chloride was removed. When the water in a gel was replaced by ethyl alcohol, Kistler referred to it as an alcogel. The gels were dried by putting them into an autoclave and raising the temperature until the pressure exceeded the critical pressure and then slowly venting the vapors in the autoclave. It was claimed that the aerogels obtained in this manner ranged from transparent to highly opalescent and occupied the same volume as the original alcogel. The density of the aerogel was varied by altering the concentration of silica in the solution. The aerogels were heated to over 700 °C without significant change in appearance. The transmittance of the material decreased when the temperature was increased to 900 °C. Thermal conductivities were determined for aerogels in granular as well as cake form. The evacuated samples of granulated aerogels had thermal conductivities of about 0.010 W m⁻¹ K⁻¹ at ambient temperatures; this value was much lower for fine granules. A change in the external load did not alter the conductivity significantly. Aerogel tiles showed smaller conductivities at 100 kPa than granular layers but the opposite trend was found at low pressures. From the changes of conductivity with internal gas pressure above 10 kPa, Kistler derived pore size diameters to be of the order of 50 nm. Aluminum acetate, which was subsequently dialyzed to form a 1% solution, was used to form the alumina gel. After gelation, the gel was allowed to dry down to the appropriate concentration. The gel was converted to an alcogel that was subsequently autoclaved to remove the alcohol. Kistler's work is reported in three patents[11,12] that were issued in 1937, 1940, and 1941.

III. Gel Preparation and General Aspects

The preparation of aerogels is still, to a great extent, an art, and much skill is required to achieve a specific end product. The next reported description of the preparation of an aerogel was for use in the IR study of silica surfaces given by Peri in 1966.[13] He hydrolyzed tetraethyl orthosilicate (TEOS) in ethanol with hydrochloric acid and obtained flat gels by allowing the gel formation to occur on a mercury surface. The methanol was slowly replaced by water, and eventually the gel plates were aged for 4 h in water at 100 °C in a closed autoclave. The gels were then slowly transferred back into a methanol solution, which was subsequently vented from an autoclave at conditions of 250–300 °C and 1200–1500 psi (8270–10340 kPa). The plates obtained were flat, transparent, and free from cracks, having dimensions of up to 1 × 3 inches (25 × 75 mm) with thicknesses of ¹/₁₆ to ¹/₈ in. (1.6–3.1 mm). The aerogels had approximate densities of 0.18 g/mL, surface areas of 800 m²/g, and pore diameters of 25 nm. The gels were purified by calcination in oxygen, with evacuation at 600 °C.

In 1968, Gilbert Nicolaon submitted his doctoral thesis to the University of Lyon on the subject "Contribution to the Study of Silica Aerogels".[14] He described in detail a variety of processes by which aerogels were made. Acid- and alkali-precipitated gels were prepared and characterized for surface area and pore size. The optical transmission properties of the aerogels formed were not reported, since the material was produced for catalytic purposes, and transparency
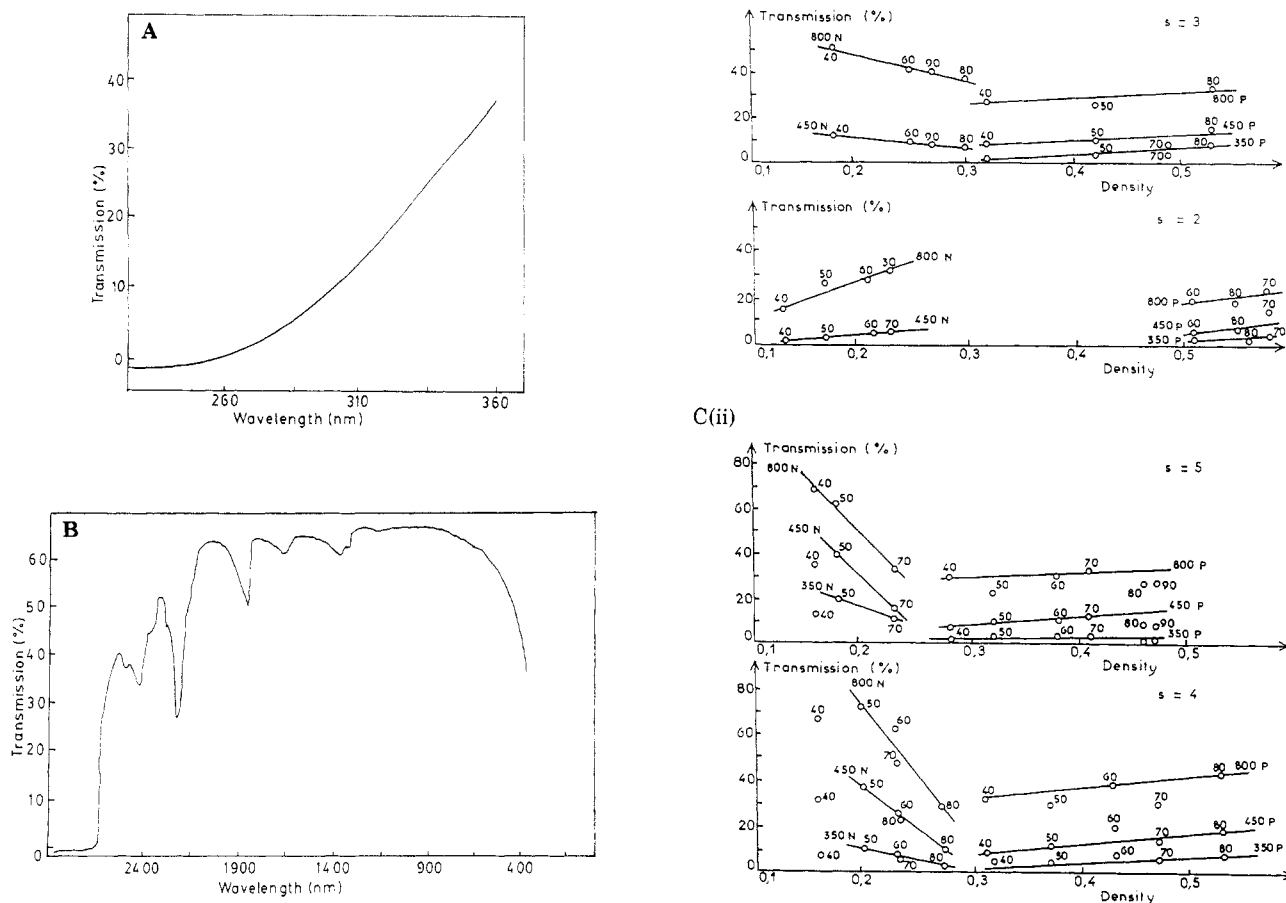
Figure 2. (A) UV transmission of a silica aerogel (density 0.16 g/mL) of 0.4-mm thickness. (B) Visible and near-IR transmission of a silica aerogel (density of 0.16 g/mL) of 0.4-mm thickness. (C) Transmission of silica aerogels at three wavelengths, 350, 450, and 800 nm, as a function of S, the ratio of moles of water to moles of methyl orthosilicate, and the resultant density. Hydrolysis conditions: N = ammonia; P = neutral. (i) For S = 2 and 3; (ii) for S = 4 and 5. Reprinted with permission from ref 18; copyright 1977, University Claude Bernard, Lyon.

was probably not of interest to Prof. Teichner, the supervisor of this work. The contents of the thesis are summarized in six papers[15] and resulted in a patent issued in 1972.[16] The preparation of alumina aerogels by Teichner and his students has also been described.[17] Again, the visual transmission properties of the aerogels were not given; the end uses of the aerogels were for catalytic studies and fundamental adsorption studies of the surface.

Teichner and his co-workers subsequently applied their method of preparing silica aerogels to the detection of Cerenkov radiation.[1] The desirability of silica aerogels as Cerenkov detectors is based on the ability to vary the refractive index of the aerogel from 1.01 up to 1.2. This essentially replaces the use of compressed gases as the detection media. The important feature of silica aerogels for Cerenkov detection lies in the transmission properties of the aerogel. This was the first time transparent monolithic pieces of aerogel were made for a specific application. The aerogels were made by the hydrolysis of tetramethyl orthosilicate (TMOS) with ammonia in a methanol solution. A large autoclave was used. A detailed description of the preparation is included in the doctoral thesis of Jean Moutel.[18] The thesis describes hundreds of experiments where the hydrolysis of the silicate was performed under acidic, basic, and neutral conditions in various solvents to form opaque as well as transparent gels of various charac-

teristics. The densities achieved varied from 0.16 to 0.66 g/mL, and the refractive index from 1.04 to 1.65. Some optical transmission results are shown in Figure 2. The factors that influenced the density of the aerogel samples were (a) the nature of the reaction medium, that is, neutral or ammonia for hydrolysis, (b) percentage of the orthosilicate dissolved in the methanol, (c) and the number of moles of water per mole of silicate used to effect the hydrolysis of the TMOS, which was varied from 2 to 6. The percentage of TMOS was varied between 40 and 100%. Over 70 different combinations of gelling conditions were studied, in most cases in triplicate, giving over 200 samples. Surface areas were determined and thermal stability was established.

The production of silica aerogels for Cerenkov radiation detectors was also described by the Swedish workers Henning and Svenson in 1981.[19] Pieces as large as 18 cm × 18 cm × 3 cm were prepared by an elaborate, detailed procedure. Again, TMOS was used in methanol with ammonium hydroxide as a hydrolysis catalyst.

Similar aerogels of silica for use as Cerenkov detectors were prepared by a Hamburg group in 1981, with samples as large as 17 cm × 17 cm × 2.3 cm.[20] The autoclaves used by these workers were 95 cm deep and had a 26 cm inside diameter. They were constructed of stainless steel as well as ordinary steel with a stainless

TABLE I. Compressive Strength of Aerogel[a]

sample	area, m^2	init thickness, mm	linear region σ_{max}, N/m^2	linear region σ_{max}, psi	linear region E, N/m^2	end of test σ_{max}, N/m^2	end of test σ_{max}, psi
C1	1.145×10^{-3}	4.21	7.69×10^5	112	2.00×10^6	6.99×10^6	1010
C2	3.360×10^{-4}	2.87	1.49×10^6	216	2.18×10^6	2.38×10^7	3450
			$1.13 \times 10^{6\,b}$	164[b]	$2.09 \times 10^{6\,b}$		

[a] Reference 5. [b] Average values.

TABLE II. Tensile Strength of Aerogel[a]

sample	area break, m^2	ultimate force, N	σ_{max}, N/m^2	σ_{max}, psi
T1	9.61×10^{-5}	0.440	4580	0.66
T2	2.13×10^{-4}	2.675	12540	1.82
			8560[b]	1.24[b]

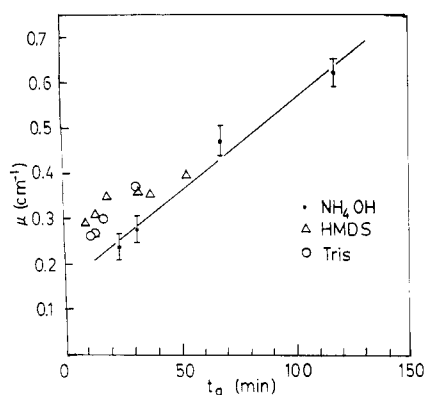[a] Reference 5. [b] Average values.

Figure 3. Transmission coefficient of aerogel samples fabricated with different gelling times t_g and measured with blue light (λ = 438 nm). The relative volumes were 2:1:4.7 silane:water:methanol. The straight line represents the points with ammonia as catalyst. The data points for HMDS and Tris have similar errors as for ammonia. Reprinted with permission from ref 20; Copyright 1981 Deutsches Elektronen-Synchrotron (DESY).

steel liner. The transmittance of the aerogel samples is shown in Figure 3, which indicates that a short gelling time is conductive to a high transmittance.

A more detailed account of the experimental methods and results related to Schmitt's work is found in his M.Sc. thesis.[5] Schmitt tested approximately 25 different catalysts to initiate the gel and concluded that tetrafluoroboric acid (HBF$_4$) was the best, and hydrofluoric acid the second best and most practical catalyst. The kinetics of gelation with hydrofluoric and hydrochloric acid were determined, and the rates of reaction and temperature coefficients were evaluated. Steady-state thermoconductivity measurements were determined by placing a 2 in. × 2 in. × 0.4 in. (50 mm × 50 mm × 10 mm) slab of aerogel between two chambers, one containing steam and the other water, and observing equilibrium temperature conditions. Schmitt also determined the compression and tensile strength of the aerogels as a function of density. Some results are summarized in Tables I and II.

Silica and alumina aerogels are also obtained from dispersing fumed silica (Cab-O-Sil)[9b] and fumed alumina (Alon) in alcohol and subsequent hypercritical drying.[9c]

Blanchard et al.[21] obtained binary aerogels such as silica-supported iron oxide (SiO$_2$-Fe$_3$O$_4$) by redispersing silica aerogel in methanol containing iron(III) acetylacetonate. The iron salt was hydrolyzed at 25 °C by

adding a calculated amount of water, and the system was heated in an autoclave to achieve hypercritical conditions (P = 150 atm, T = 275 °C). A variant of this method involved only decomposition of the iron salt in the redispersed system under hypercritical conditions without going through the hydrolysis step. Similar aerogels were prepared by using Al$_2$O$_3$, TiO$_2$, or ZrO$_2$ in place of SiO$_2$. Sayari et al.[22] studied the catalytic properties of NiO on six combinations of SiO$_2$, Al$_2$O$_3$, and MgO.

Central to the production of advanced microporous materials is the need for a detailed understanding and control of the chemical processes that occur during gel formation.[23]

General aspects of the chemistry of metal alkoxides, which make excellent molecular precursors for a variety of inorganic oxides of high purity, have been reviewed.[24-26] The ability of the alkoxides to form homogeneous solutions in a large variety of solvents and in the presence of other alkoxides or metallic derivatives makes it possible to achieve homogeneity at the molecular level. The parameters governing the hydrolysis of the alkoxides and polymerization were examined. Modulation of the rheological properties of the sol by controlling the hydrolysis rates enables one to obtain films, coatings, fibers, and various body-shaped materials.

The sol-gel process (Figure 4) describes the transition of a system from liquid, mostly colloidal, into a solid, gel phase. This reaction route can start from two basically different systems—gelation may proceed due to condensation of colloidal particles (by sol destabilization), cluster growth, and cross-linking of polymeric molecules.[23]

Hydrolysis

$$MOR + H_2O \rightarrow MOH + HOR$$

Condensation

$$MOR + HOM \rightarrow MOM + HOR$$

$$MOH + HOM \rightarrow MOM + H_2O$$
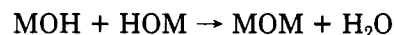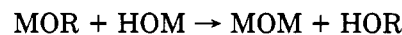
where M = metal or Si and R = alkyl group. Both reactions are catalyzed by acids and bases. However, they also proceed under neutral conditions. The rates for hydrolysis and gelation are strongly pH dependent. To produce fairly homogeneous solids, network-forming components such as Si, main group metals, early transition metals, or lanthanides, usually in the form of alkoxides, should be present. These accommodate the formation of a three-dimensional network, typical of a condensation reaction. Acid catalysis leads to a more
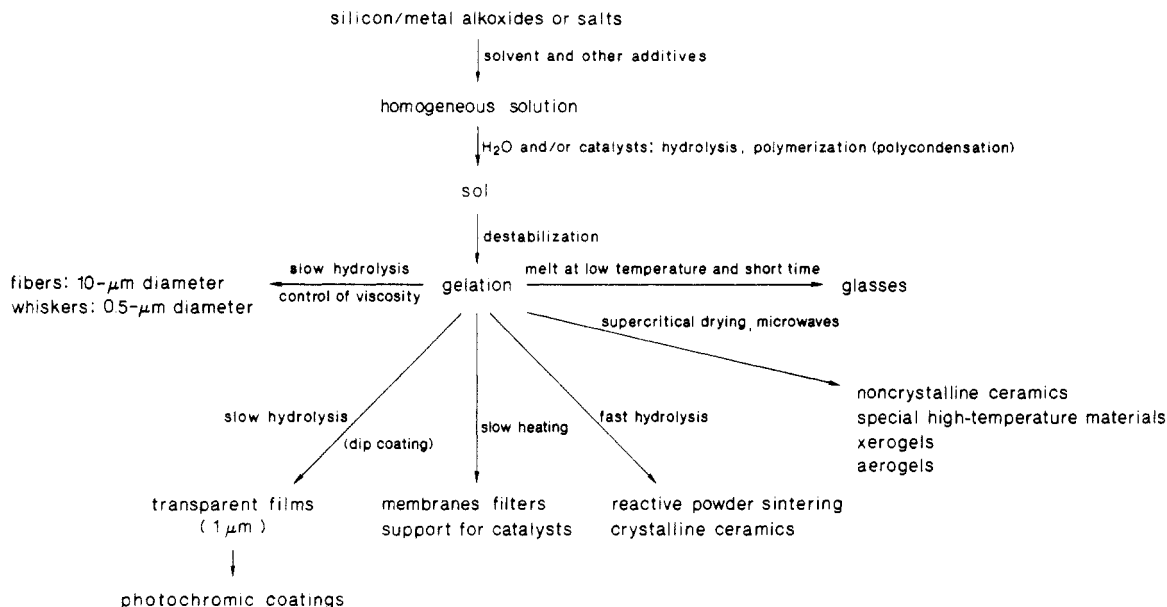
silicon/metal alkoxides or salts

solvent and other additives

homogeneous solution

H_2O and/or catalysts: hydrolysis, polymerization (polycondensation)

sol

destabilization

fibers: 10-μm diameter   slow hydrolysis   gelation   melt at low temperature and short time   glasses
whiskers: 0.5-μm diameter   control of viscosity

supercritical drying, microwaves

slow hydrolysis   slow heating   fast hydrolysis

(dip coating)

noncrystalline ceramics
special high-temperature materials
xerogels
aerogels

transparent films   membranes filters   reactive powder sintering
(1 μm)   support for catalysts   crystalline ceramics

photochromic coatings

Figure 4. The sol-gel process.

polymeric form of gel with linear chains as intermediates. Base catalysis yields colloidal gels. Gelation occurs by cross-linking of the colloidal particles according to the reaction

$$-O-M-OH \ + \ HO-M-O- \ \longrightarrow$$

$$-O-M-O-M-O- \ + \ H_2O$$
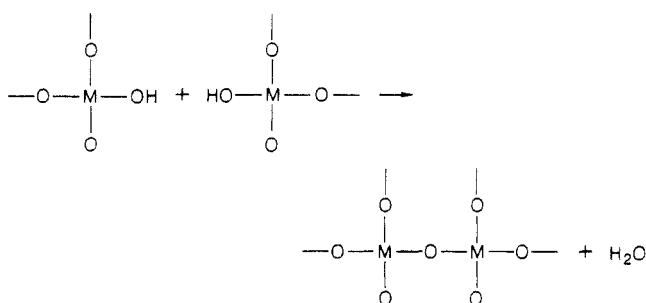
It is evident that hydrolysis and condensation conditions set the primary structures of the gels and thereby influence further steps. Alkoxides are very sensitive to water, so hydrolysis is possible for a large variety of compounds. Organic network formers or modifiers can be introduced by using organically substituted silico esters as starting compounds, $R'_nSi(OR)_{4-n}$, where R' is an organic functional group and OR is a hydrolyzable group. The reaction path, though it appears to be simple, is a complex one, since the single steps are overlapping.

The various factors governing the hydrolysis–polycondensation reactions[24] are (i) the degree of hydrolysis, $h = [H_2O]/[M(OR)_n]$, with $h < n$ leading to fibers, chains, and coatings and $h > n$ leading to gels and three-dimensional polymers; (ii) the nature of the metal and polarity of the M–O–C bond; (iii) n, the number of alkoxo groups, the rate decreasing with an increase in n; (iv) the nature of the alkoxo group R (this governs the molecular complexity, increases the rate with chain lengthening, and controls the sensitivity to hydrolysis (tertiary R > secondary R > primary R, OPh > OR > $OSiR_3$, OPh > o-OC_6H_4X > p-OC_6H_4X)); (v) pH; (vi) solvent and dilution; and (vii) temperature.

Upon gelation, viscosity increases sharply until the gel point is reached. The structure of the gel, however, may still change; i.e., aging depends on temperature,
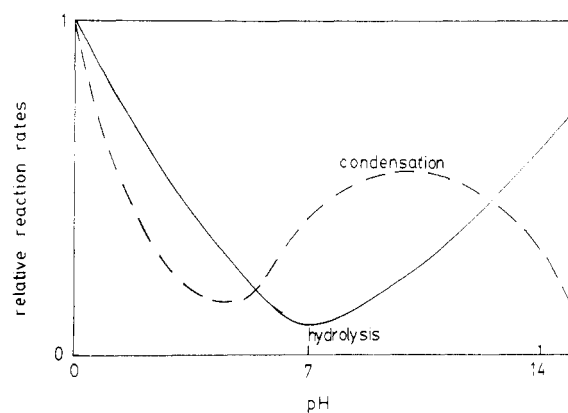
Figure 5. Hydrolysis and condensation of TEOS as a function of pH. Reprinted with permission from ref 23; copyright 1986 Springer-Verlag.

solvent, and pH. The effect of pH on the relative reaction rates of hydrolysis and condensation of TEOS is shown in Figure 5. The condensation reaction starts at a late stage in the case of acid catalysis, but with base catalysis condensation starts relatively early. The hydrolysis and condensation reactions of monomeric alkoxysilanes and organoalkoxysilanes were reviewed by Brinker.[27]

Schmidt and Scholze[23] discussed the sol–gel process for nonmetallic inorganic materials. Mechanisms of hydrolysis and condensation and problems associated with maintaining monolithicity were discussed. Mention was made of network modifiers; e.g., the introduction of low-valent cations (such as alkali ions) decreases bond strengthening and leads to lower porosities. Organic network modifiers can also be incorporated into the inorganic network by the sol–gel process—the organic grouping can be introduced by using an organosilicoester. The sol–gel process can be modified to include a large variety of components including network formers (e.g., Ti, Zr, and Al) and network modifiers such as organics and dopings.[28] The chemical modification achieved by reacting metal alkoxides (Ti, Zr, Ce) with a variety of chemical additives containing nucleophilic hydroxy groups leading to ad-

dition and substitution reactions has been discussed by Sanchez et al.[29] Substitution occurs when highly electrophilic metal alkoxides react with nucleophilic hydroxylated ligands. Alkoxy groups are then replaced by new ligands that are more or less easily removed upon hydrolysis. A metal oxide is still obtained when the new ligand is hydrolyzable while a mixed organic-inorganic network is formed when the metal–ligand bond cannot be broken by hydrolysis. When $Ti(OBu^n)_4$ and glycol were used, $Ti-OH_2CCHOHCH_2O-Ti$ and $Ti-O-Ti$ bridges could be formed, and transparent orange monolithic gels were obtained. The process involving organically modified silicates (ORMOSILS) has wide material development potential and has been further reviewed by Schmidt.[30]

Another preparation of a silica aerogel for use as a Cerenkov detector was described using 0.04 M NH_4OH and cooled preboiled solutions.[31] Several sol–gel systems involving oxides other than SiO_2 have been described:

TiO_2-SiO_2: TiO_2-SiO_2 was used for low thermal expansion substrates[32,33] (glass for optical instruments, fibers, and films), and $Na_2O-Al_2O_3-CaO-TiO_2-SiO_2$[34] was used in glass ceramics for radioactive waste immobilization. The importance of control of hydrolysis rate of titanium alkoxide in the preparation of high titania content (20–50%) transparent, monolithic TiO_2-SiO_2 glass was discussed and demonstrated by Lirong et al.[35]

SiO_2-GeO_2: Raman spectral studies[36] of a number of gels prepared from different alkoxysilanes at different pHs after thermal treatment at different temperatures showed the presence of Si–OH and Ge–OH groups. The silica-rich gels prepared at pH 2–3 using $Si(OCH_3)_4$ and $Ge(OC_2H_5)_4$ showed greater tendency to retain Si–OH groups than the corresponding gels prepared with $Si(OC_2H_5)_4$ and $Ge(OC_2H_5)_4$ when heated at various temperatures up to 1300 °C. GeO_2-doped silica glass[37] for optical fibers were obtained by hydrolysis of a solution of tetraethoxysilane and tetrabutoxygermanium in ethanol. The generation of GeO_2 crystal depended on the ammonia–water content in the sol.

ZrO_2 (Refractory and Catalyst Support): Hydrous zirconia gels obtained by bubbling ammonia through an aqueous solution of zirconyl oxychloride became more microporous with an increase of pH, while heat treatment led to collapse of the structure, which became nonporous at 400 °C.[38] The contributions of both evaporation–condensation and surface diffusion mechanisms in the sintering of ZrO_2 gels prepared by hydrolysis of $ZrCl_4$ and zirconium alcoholates have been studied.[39] While surface diffusion tended to produce an agglomeration of primary particles to form micelles of larger size with a corresponding reduction in specific surface, the vapor transport mechanism led to a reduction in the pore volume as the material was deposited on the concave pore walls. Gravimetric techniques[40] were employed to characterize the irreversible textural changes in hydrous zirconia gels prepared by hydrolysis of aqueous zirconyl chloride by ammonia. Water played a key role in the aging mechanisms of microporous hydrous zirconia gels—the extension of the microporous network to facilitate the removal of trapped water molecules and the closure of the micropores in a poorly ordered hydrous oxide system. The

textural studies[41] of ZrO_2 xerogels prepared by hydrolysis of $ZrCl_2$ and zirconium alcoholates in water, propanol, and butanol revealed a marked influence of the starting chemical on the texture of these materials and their resistance to sintering. The results seemed to exclude any appreciable influence of the surface tension of the preparation medium on the porosity and on the ease of capillary collapse in the oxides studied. ESR and X-ray studies[44] were made on ZrO_2 gels prepared by hydrolysis of zirconyl oxychloride and zirconium nitrate to understand the formation of different crystalline phases. The adsorption and textural studies on ZrO_2 gels[45] indicated that microporosity (0.2 cm^3/g) was sensitive to both temperature and pH of precipitation; high pH and low temperature are the best conditions to get the most microporous samples. ZrO_2 coating films[43,49] were prepared from hydrolysis of zirconium n-butoxide with moisture by the dipping method, and the optimal transmittance of the films had been found to be very sensitive to humidity whereas transparency was achieved below 20% relative humidity. Using β-dicarbonyl ligands such as acetylacetone and ethyl acetoacetate, Yamada[42] was able to prevent undesirable precipitation of tetrabutoxyzirconium and was able to obtain transparent and alkali-resistant coatings curable at room temperature.

$TiO_2-Sb_2O_3$: Thin TiO_2 films with various amounts of Sb_2O_3 were prepared for photoelectrochemical studies.[46] The photocurrent of these films increased to ~25 mA cm^{-2} by the addition of 0.5 mol % of Sb_2O_3 but decreased sharply with further increase in doping concentration.

Al_2O_3: Solution and solid-state ^{13}C NMR, ^{27}Al NMR, X-ray powder diffraction, and scanning electron microscopy were used to characterize Al_2O_3 obtained by hydrolysis of aluminum propionate.[47] The results indicated that sonicated dried powder was crystalline γ-Al_2O_3 while the unsonicated sample was amorphous and crystallized at 800 °C with the Al_2O_3 structure. Al_2O_3 sols prepared by hydrolyzing $AlCl_3·6H_2O$ were studied by TEM to characterize the shape of the particles in the sol and relate to rheology and fiber-drawing behavior of the sols.[48] It was found that fibers could be drawn in the viscosity range of 1–100 Pa s from the sols in which long-shaped particles were found.

Li_2O-SiO_2: Transparent, amorphous films in the system Li_2O-SiO_2[50] were prepared by hydrolyzing silicon tetraethoxide and lithium alkoxide. The electrical conductivity for the films with relatively small amounts of lithium increased with an increase in the heat treatment temperatures below the crystallization temperature.

(Li or K or Na)$_2O$-(Ti or Zr)O_2-SiO_2-P_2O_5: A variety of inorganic oxides[51] were obtained by the general sol–gel method using hydrolysis of mixtures of $Zr(C_3H_7O)_4$ or $Ti(C_4H_9O)_4$, $Si(C_2H_5O)_4$, $PO(C_4H_9O)_3$, and $Na(C_4H_9O)_4$, $Li(C_4H_9O)$, or $K(C_2H_5O)$ in ethanol. Depending on the method of treatment, these materials could have different forms: monolithic xerogels, glasses, fibers, films, and ceramics.

CeO_2: Thin films of ceria gels were obtained by dipping stainless steel substrates into ceria sol.[52]

CeO_2-TiO_2: A transparent, yellow coating film of CeO_2-TiO_2 was prepared from titanium isopropoxide and cerium chloride by the sol–gel dip-coating method.[53]

Films of 0.3-μm thickness were obtained per dipping, and the relation between the number of dippings and thickness as well as the number of dippings and brightness of the yellow color were almost linear.

SnO_2: Stannic oxide gels[11b] were prepared by hydrolyzing a solution of $SnCl_4 \cdot 5H_2O$ by placing it in a dialyzer made of cellophane and then suspending it in a large volume of flowing distilled water for 24 h, after which $Sn(OH)_4$ would set into firm jelly. The jelly, after washing several times with methanol to free any water, was hypercritically dried with respect to methanol to yield a transparent aerogel for catalytic use.

V_2O_5: Transition-metal oxide gels can be obtained, through a polycondensation process, by acidification of aqueous solutions. The semiconducting properties of V_2O_5 gels[6] are useful for antistatic coatings or electrical switching devices. V_2O_5 gels are also used as catalysts.

Vanadium pentoxide gels are also prepared[54-58] by polymerization of vanadic acid. Polyvanadic acid solutions are prepared by ion exchange in a resin from sodium metavanadate solution. A reversible sol-gel transition occurs for vanadium concentrations around 0.1 M. Most of the water evaporates readily at room temperature, yielding a xerogel ($V_2O_5 \cdot 1.6H_2O$). Upon heating, all the water is removed and crystallization occurs at 350 °C, yielding orthorhombic V_2O_5.

WO_3: WO_3 gels,[6,59] important for photochromic and electrochromic properties, are obtained by passing an aqueous solution of sodium tungstate through a cation-exchange resin (Dowex 50, WX2, 100–200 mesh). A clear, yellow solution is obtained that progressively becomes turbid and turns into a gel. The yellow gel on drying at room temperature becomes a xerogel powder.

UO_2: UO_2 microspheres[60] for nuclear fuel material were produced by gelation of solutions containing uranyl nitrate, hexamethylenetetramine, and urea.

ThO_2-UO_2:[61] Nitrate-stabilized thoria sols were prepared by mixing at 80 °C with the desired composition of uranyl nitrate. The pH was adjusted by addition of nitric acid or ammonia. The sols were studied by electron microscopy for fabrication of spherepac, mixed-oxide nuclear fuels.

Sc_2O_3: Scandia gels were prepared[62] by slow thermal decomposition of $Sc(OH)_3$ at a constant rate and a low pressure of water vapor (0.04–0.09 Torr). Structural and phase changes were studied by TGA, SEM, and XRD.

$MgO-Al_2O_3$: Transparent, noncrystalline, monolithic $MgO-Al_2O_3$ gel[63] was prepared by the sol-gel process by polymerization of $Al(OC_4H_9)_3$, acetylacetone [$CH_2(COCH_3)_2$], and magnesium acetate tetrahydrate [$Mg(OOCCH_3)_2 \cdot 4H_2O$] in an ethanol–isobutyl alcohol mixture in the presence of HNO_3 as a catalyst. After heat treatment in an oven transparent monoliths were obtained.

$SnO_2-Sb_2O_3$: Amorphous xerogels were prepared[64] by the sol-gel route corresponding to the same chemical composition as in the semiconducting glaze of industrial high-voltage insulators [66% glassy phase (70% SiO_2, 9% Al_2O_3, 4.5% $(K,Na)_2O$, 9% CaO, 7.5% ZnO) and 33% SnO_2 + Sb_2O_5 with SnO_2/Sb_2O_3 = 97/3]. The thermal behavior of the xerogels was studied by X-ray diffraction line-broadening analysis, SEM, and energy-dispersive analysis. The chemical instability of gel-derived semiconductors above 1100 °C was dis-

cussed in terms of redox reactions involving Sn and Sb species.

Recently, Russo and Hunt[65] reported the preparation of a transparent base-catalyzed TEOS aerogel using NH_4OH and NH_4F as catalysts. Russo and Hunt, using polar nephelometry, reported that the base-catalyzed TMOS system provides better optical quality gels than the acid-catalyzed TEOS system.

Tewari[66] and Gowda[67] have prepared silica aerogels using CO_2 as the supercritical fluid. Since CO_2 has a lower critical temperature (T_c = 31 °C, P_c = 73 atm) than methanol (T_c = 240 °C, P_c = 78 atm), the venting of solvent as a gas is experimentally easier for CO_2. However, complete exchange of the methanol for CO_2 must occur.

Italian investigators Pezzo et al.[68] studied the influence of the variation of the H_2O/TEOS molar ratio (between 5 and 50) on the microporosity of xerogels produced by hydrolysis of TEOS in the presence of C_2H_5OH and HCl. The gels were allowed to stand at 60 °C and dried in vacuo (P = 0.01 Pa) at 22 °C. The adsorption isotherms were determined at −196 °C with nitrogen and at 25 °C with water. The specific surface area, total pore volume, and the mean radius of mesopores in the micromesoporous silica gels increased with H_2O/TEOS molar ratio, the dependence of the first two parameters being linear. The volume of micropores appeared to be independent of the H_2O/TEOS ratio. Specific surface area of the sample prepared with a H_2O/TEOS molar ratio of 50 reached a value of 665 m^2/g, as determined by the BET method with nitrogen. Recently, Avnir and Kaufman[69] produced alcogel from hydrolysis of TMOS without using methanol as a mutual solvent. The alcohol released during the reaction was sufficient to convert the initially biphasic system (H_2O/TEOS = 4:1) into a homogeneous one, resulting in a transparent, porous xerogel after air-drying.

The kinetics of silical polymerization was studied by Weres et al.[70] The kinetics of the sol-gel transition was discussed by Klein and Garvey,[71] who also obtained[72] monolithic dry gels that were amorphous and transparent. However, densities were high (about 1.6 g/mL) and air-drying time was of the order of a month. The object of the work was to obtain a low-temperature glass, formed by fixing the gel at high temperature. Much has been reported on the sol-gel route to low-temperature glasses.

Abe and Misono published a series of papers summarizing their study of the polymerization of silicic acid.[73] They have further shown[74] how it is possible to extract the polymeric acid from water using tetrahydrofuran (THF). The polymer can then be transferred to methanol, and slow evaporation can yield a transparent monolithic gel. No densities were reported. This approach, which starts with water–glass, seems to promise an inexpensive method of preparing transparent xerogels.

The polymerization of silicic acid, using sodium silicate and tetraethyl orthosilicate, was studied by Bechtold et al.[75] The kinetics were studied, and molecular weights (M_w = 7200 to 1.7 × 10^6 Da) were determined. The gels were used to prepare fibers that had remarkable properties.

The kinetics of gelation of tetramethylalkoxide sols were studied by measuring viscosities.[76] Gelling time

decreased and the viscosity increased with increase of the alkoxide content. In neutral medium the same behavior was observed with increasing water content but in acidic medium the gelling time showed a minimum and viscosity a maximum when the water:alkoxide molar ratio was between 2 and 4; below 4, hydrolysis was incomplete and above 4, the excess water played the role of a solvent isolating and diluting the polymers, thereby decreasing viscosity.

In the preparation of oxides by the sol–gel process, viscosity and molecular weight of species increase with time. Pope and Mackenzie[77a] utilized this observed viscosity–time relationship to elucidate the structural evolution of gels and developed two theoretical models—one for nearly linear growth (applicable to HCl-catalyzed silica gel) and another for fractal growth (applicable to HF-catalyzed silica gels).

Temperature dependence studies[77b] of the gelation of silicon alkoxides in corresponding alcoholic solutions with HCl, HF, or no catalyst and water showed that gelation time was related to the increase of temperature by an Arrhenius relation. The activation energies for gelation ranged from 9.1 to 19.5 kcal mol^{-1} for the temperature range 0–70 °C.

Several papers on diphasic xerogels[78–81] described the preparation of Si/Al, Si/Ag, and other mixed-oxide systems. The gelling time of a 10% tetramethoxysilane solution in water was shown to be fast almost up to pH 10 (except for pH 1–3, the gelling is slightly slowed); gelling times were 5 days at pH 11 and 10 days at pH 12.[82]

The structure of solid phases in TiO$_2$ and ZrO$_2$ gels, obtained from inorganic and organic sources, was studied by Komarneni et al.[83] X-ray diffraction (XRD) and selected-area electron diffraction (SAED) failed to show any crystalline Ti and Zr hydroxides. Both gels were porous.

Kokubu and Yamane[84] discussed the extraordinary thermal and chemical stability of porous glass ceramics of the TiO$_2$–SiO$_2$ system. Porous glass ceramics containing both anatase and rutile had thermal expansion coefficients of $(40-55) \times 10^{-7}$ K^{-1} in the 0–700 °C range. They remained porous up to 1000 °C, while the pores of high-silica porous Vycor collapsed completely. They attribute the high thermal stability to a high viscosity, resulting from dispersed crystallites of anatase and rutile in the skeleton. Most of the anatase in the skeleton was transformed to rutile during heat treatment at 900 °C, but some remained untransformed even after 6 h.

Tewari, Hunt, and Lofftus[85a] described their work at Lawrence Berkeley Laboratories, where they hydrolyzed Si(OC$_2$H$_5$)$_4$ with NH$_3$ and NH$_4$F catalysts. Ethanol was used as the mutual solvent. A factorial design method was used to choose the experimental parameters, enabling them to reduce the number of experiments required to reach logical conclusions. The concentrations of alkoxide, water, alcohol, NH$_4$F, and NH$_3$ were simultaneously varied. The resulting aerogels were either equivalent or better in quality than those produced with the more toxic TMOS as the starting material. Samples were dried with CO$_2$ at 40 °C and 8000 kPa.[85b] Light scattering, optical spectroscopy, rheology, system pH, shrinkage during drying, transmission and scanning electron microscopy (TEM, SEM), and surface area measurements were used for sample characterization and optimization.

Zarzycki and Woignier[86] discussed their work, which was performed at the CNRS glass laboratory in Montpellier and involved SiO$_2$ and other SiO$_2$–B$_2$O$_3$ and SiO$_2$–P$_2$O$_5$ binary system and SiO$_2$–B$_2$O$_3$–P$_2$O$_5$ ternary system aerogels. Aging at room temperature for 3 weeks and at <50–60 °C seemed to improve monolithicity. Ternary systems revealed strong crystallinity that increased with B$_2$O$_3$ and P$_2$O$_5$ content. The crystalline phase was identified as BPO$_4$. The optical transmission of the aerogels was found to be strongly dependent on the initial composition of the gelling solution. Because of the greater proportion of larger pores (>100 nm in diameter) in the gels prepared from more dilute neutral solutions of TMOS (20 and 40 vol %), these gels were less translucent than the ones prepared from 60 vol % TMOS solution. On the other hand, silica aerogels prepared from 20 vol % TMOS with ammonia as catalyst ($N = 0.5$) showed great improvement in transmission characteristics, which approached that of vitreous silica. This improvement was attributable to the presence of a large proportion of small pores (<100 nm in diameter). The SiO$_2$–20 mol % B$_2$O$_3$ gel showed uniform transmission between 12 500 and 50 000 cm^{-1}, while the SiO$_2$–15 mol % P$_2$O$_5$ gel cut out at around 35 000 cm^{-1}. All of these gels were dried under hypercritical conditions. They discussed how aerogels were used to produce optical-quality glass. Optical properties and sintering behavior were studied for the gel–glass transformation.

Brinker et al.[87] discussed the synthesis of borate-based aerogels in the binary system xLi$_2$O–$(1 - x)$B$_2$O$_3$. LiOCH$_3$ dissolved in methanol was diluted with 2-methoxyethanol and hydrolyzed. The solution was added to the requisite volume of tri-n-butyl borate to obtain molar compositions xLiO$_2$–$(1 - x)$B$_2$O$_3$, where x varied from 0 to 0.4. Polymer growth in solution was followed by SAXS, and the fraction of four-coordinated boron was determined in the original solutions, aged solutions, and gels using ^{11}B NMR. Structural information on the molecular scale was obtained from FTIR. The gels were dried under hypercritical conditions using CO$_2$ at 40 °C and 8270 kPa. The aerogel microstructure was examined by SEM. It was concluded that in order to grow stable polymeric species, both a critical hydrolysis ratio and an alkali ratio must be exceeded: [H$_2$O]/[OR] $\geq$ 0.44 and $x \geq 0.2$, respectively. Only primary units containing at least one four-coordinated boron appear to be stable in solution. Polymer growth occurs by linkage of these primary units at tetrahedral boron sites. At least one four-coordinated boron is required in B–O–B linkages between primary units. The borate network is very susceptible to dissociation reactions, which promote depolymerization of the network. Since this depolymerization is enhanced at higher temperatures and pressures, amyl acetate ($T_c = 326.1$ °C, $P_c = 28$ atm) was exchanged with liquid CO$_2$ before supercritical drying. This process had no detectable shrinkage. IR studies indicated that the gel was weakly polymerized compared to glass. Both SEM and TEM micrographs indicated that gelation may occur by a random aggregation of almost spherical polymeric clusters, which is similar to gelation in base-catalyzed systems. The agglomeration of such silica spheres is
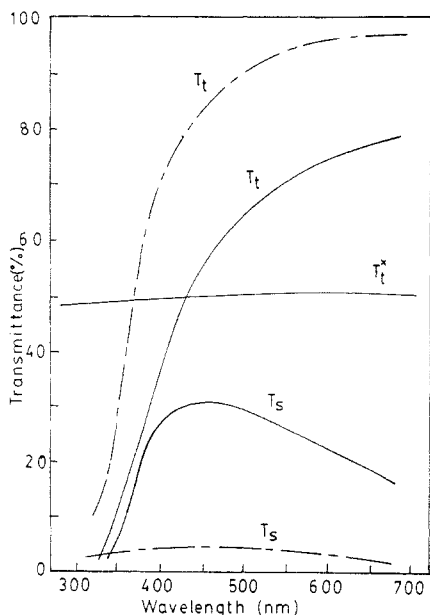
Figure 6. Total (T_t) and scattered (T_s) transmittance of 2-mm-thick specimen. Solid line represents dry stage; dash–dot line represents water-impregnated condition. Also shown is T_t of a dense transparent commercial alumina. Reprinted with permission from ref 89; copyright 1975 Americal Ceramic Society.

Figure 7. (A) Transmission spectrum of base-catalyzed aerogel (4 mm thick) prepared by CO_2 supercritical drying. (B) The spectrum after the sample was heated in air at 250 °C for 4 h. (C) The spectrum after the sample was heated to 500 °C for 12 h. (Curve C is not drawn below 600 nm because of clarity but follows closely curve B in this region.) Reprinted with permission from ref 85a; copyright 1986 Springer-Verlag.

responsible for the structure of opals.[88]

Though Teichner had reported on the preparation of alumina aerogels as early as 1970, he gave no consideration to the transparency of the materials so produced.[17] In 1975, Yoldas reported on the preparation of transparent porous alumina xerogels made by hydrolysis of aluminum alkoxides.[89,90] It is interesting to note that the preparations by Yoldas do not involve venting of the solvent in an autoclave, but rather the direct thermal heating of the transparent gel to high temperatures after an initial drying period. Typical transmittance curves are shown in Figure 6 for a 2-mm-thick sample. The samples had 63% open volume and were prepared from an alumina sol.[91] The Yoldas work is summarized in two patents dealing with the formation of the transparent alumina material.[92,93]

IV. Structural Aspects

Various modern analytical techniques have been employed to study the structure of aerogels. For pore size distribution, Hg porosimetry and adsorption–desorption of N_2 at low temperatures have been used. Results indicate that aerogels have a pore diameter distribution that extends from the nanometer to micrometer range.

A high-resolution electron microscopic study of silica aerogels has shown that the aerogel network consists of particles 10 nm in diameter. ESCA and Auger spectroscopy showed the particles to be pure SiO_2.[94,95]

Tewari et al.[96] described their investigations of microstructural properties of transparent silica aerogels with SEM and TEM. Both acid-catalyzed and base-catalyzed TEOS and TMOS aerogels were investigated. The gels were dried both by high- and low-temperature (alcohol and CO_2) supercritical drying. Optical transmission spectra (Figure 7) in the UV/vis/near-IR (200–3200 nm) region were presented. Transmittance improved on heating up to 500 °C. The rising part of the curve between 200 and 800 nm is due to scattering;
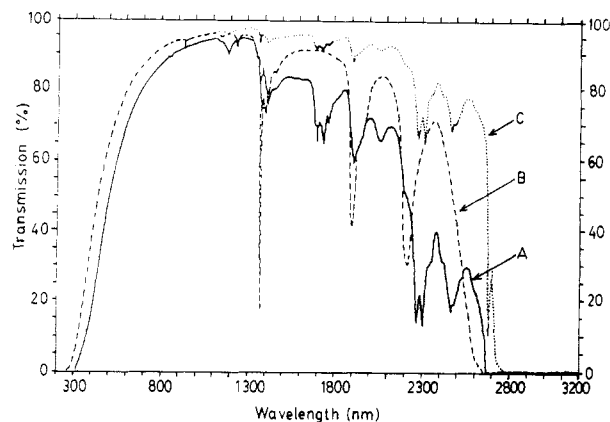
after heating to 300 °C, the curve is shifted to lower wavlengths. This is attributable to either a decrease in pore size or a decrease in the average index of refraction. When the data are analyzed for Rayleigh scattering, the characteristic size of the scatterer is found to be 8 nm, which is larger than the value of 5 nm for particle size obtained from TEM studies. Acid-catalyzed aerogels were found to be denser than the base-catalyzed aerogels. Their pore structure reflected this while the particle sizes were similar. The average void size was calculated to be ~40 nm. The surface areas of the acid- and base-catalyzed gels were between 890 and 960 m²/g, and the calculated particle size was between 2.9 and 3.1 nm for both CO_2 and high-temperature supercritical drying. Studies of light scattering during gelation indicated distinct differences between acid- and base-catalyzed gels. Base catalysis produced relatively large particles. The pore size distributions were also found to be different between the acid- and base-catalyzed systems.

Schuck et al.[97] studied the pore size distribution on aerogel samples using BET gas adsorption–desorption with N_2 at 77 K and SAXS. From BET data for three samples of densities 275, 145, and 105 g/L, the specific pore volumes were 3.16, 6.42, and 9.05 cm³/g, respectively. For these aerogels, the largest pore volume fraction (up to 90% for low-density samples) was found to be above the 60-nm-diameter range, whereas from Rayleigh scattering an upper value of pore size dimension of 200 nm was estimated. SAXS data indicated the most frequent particle diameter to be in the range of 5–6 nm (Figure 8).

The microstructure of silica-based aerogel was studied by Lampert et al.,[98] using high-resolution electron microscopy. The samples were acid-catalyzed TEOS aerogel supercritically dried at 270 °C and 12 MPa. The chemical analysis of the samples was done with a scanning Auger microscope and ESCA. The studies revealed that the silica aerogel consists of a network of amorphous stoichiometric silica clusters with an average size of ~10 nm. The aerogel transformed readily under an intense electron beam—the sizes of the particles increased to 20–50 nm and appeared to be stable with time after the transformation. The structure of the
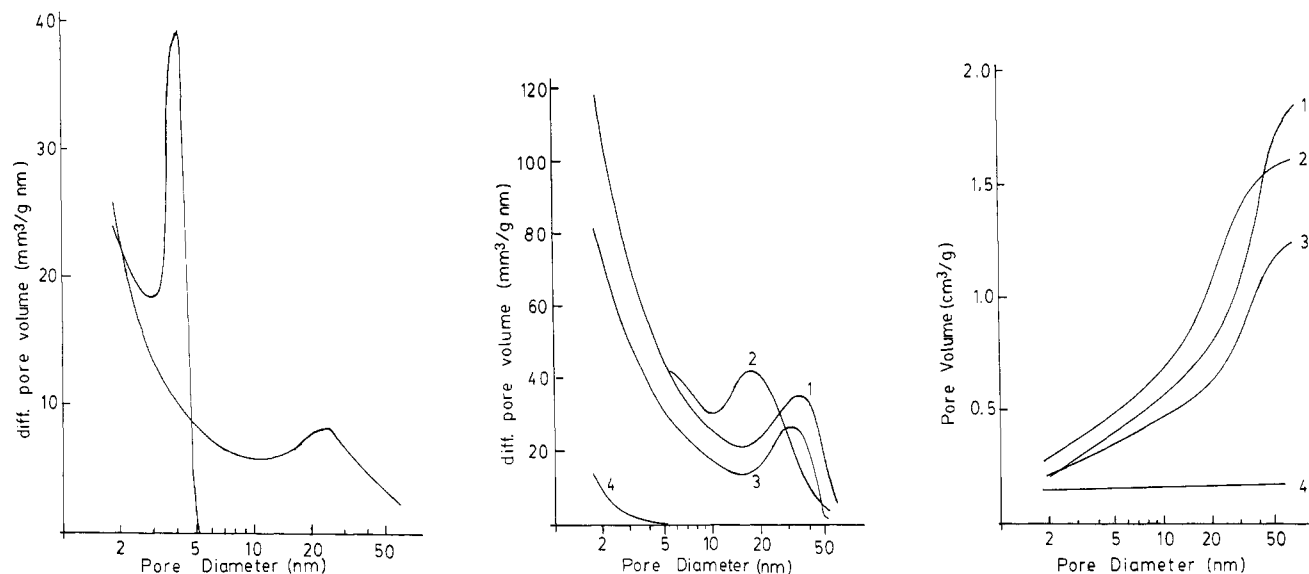
Figure 8. (a) Pore size distribution for silica gel with well-defined pore size diameter of 4 and 30 nm. (b) Pore size distribution for aerogel (samples 1–3) and for silica fiber. (c) Cumulated pore volume represented by adsorbed liquid N_2 volume per sample mass for aerogels (samples 1–3) and silica fiber. Reprinted with permission from ref 97; copyright 1986 Springer-Verlag.

TABLE III. Apparent Density ρ_a, True Density (Density of Skeleton) ρ_t, Specific Pore Volume v_p, and Porosity π for Different Aerogels[b]

sample	ρ_a, g cm^{-3}	ρ_t, g cm^{-3}	v_p, cm^3 g^{-1}	π, %
1	0.133	2.44	7.11	94.5
2[a]	0.205	1.87	4.34	89.0
3[a]	0.240	1.99	3.66	88.0
4	0.230	2.09	3.86	88.5
5	0.287	1.93	2.97	85.1

[a] Pellets. [b] Reference 99.

transformed cluster was amorphous as determined by HREM.

Broecker et al.[99] studied the structure of silica aerogel pellets at BASF. Pellets having apparent densities ranging from 0.133 to 0.287 g/mL were studied by mercury porosimetry and BET N_2 adsorption studies (Table III).

Gronauer et al.[100a] investigated mechanical and acoustic properties of silica aerogel. Longitudinal sound velocity varied between 100 and 300 m/s for aerogels of densities between 70 and 300 g/L. Compared to silica glass, an aerogel has an extremely small Young's modulus (10^6–10^7 N/m^2) and therefore can be compressed very easily. Aerogels consisting of primary SiO_2 particles a few nanometers in diameter that are interconnected by tiny necks 1 nm in diameter have a mechanically soft and elastic structure and thus have potential as a new acoustic material. Potential applications of aerogels include sound isolation at high temperatures, use in acoustic delay lines, and use as an acoustic antireflecting $x/4$ layer in piezoactive material.

Mechanical and elastic properties of silica aerogels with densities ranging from 0.1 to 0.4 g/mL were studied[100b–d] by SAXS and Brillouin scattering. The results demonstrated the fractal nature of these materials. The mechanical properties were followed as a function of bulk density, and aerogels with porosities 95% revealed a maximum flexural strength lower than 10^{-2} MPa. The elastic properties were analyzed in terms of a percolating system.

The skeletal densities, macroscopic densities, and fractal dimensions of aerogels with densities in the range of 0.07–0.4 g/mL were studied.[101,102] The skeletal densities varied between 1.7 and 2.2 g/mL. Woignier[102] used helium pycnometry for skeletal density measurements and found that the bulk and the skeletal densities varied as a function of alkoxide concentration, pH, and densifying treatment. With respect to skeletal densities, no significant differences between xerogel and aerogel were apparent.

The dielectric response studies[103] on silica aerogels between 1.6 and 300 K and frequencies between 50 and 10^5 Hz showed that the dielectric constant was practically constant between room temperature and 100 K but smaller than of fused silica. A sharp decrease was observed near 35 K and accompanied by a large loss peak.

Brillouin scattering studies on silica aerogels by Courtens et al.[104] were consistent with a fractal description that the samples form single infinite clusters. dos Santos et al.[105] using SAXS, BET, density, and TEM techniques found that all structures of silica aerogels could be described as mass fractals. The results confirmed the existence of structural units forming the SiO_2 matrix having average size of 1.35 nm (basic), 0.85 nm (neutral), and <0.7 nm (acidic). Hypercritical drying did not alter the overall structure though it did smooth the surface of the structural units slightly. The main fractal features of the aerogels were similar to the ones corresponding to the secondary structure of the precursor gels. Raman scattering studies[106] showed that acid- and base-catalyzed silica aerogels had dynamical fractal behavior between 10 and 180 cm^{-1}.

Infrared absorption studies on alkoxide gels showed the effect of added fluoride on Si–OH formation.[107] The alcogel structure (after complete water exchange) was characterized by thermoporometry and shown to consist of lightly connected cylindrical pores of 2.5-nm radii.[108] The shear modulus of silica gels was shown to be dependent on the concentration of silica in the alcogel.[109]

The hydrolysis of TEOS to gel formation was followed by ^{1}H NMR.[110] The signal of residual CH_2 and

CH_3 in the gel dried for 4 months was present even when the H_2O/TEOS mole ratio was 6. These organic groups disappeared when the ratio was increased to 15.

Sindorf et al.[111] used solid-state ^{29}Si NMR experiments, employing cross polarization (CP) and magic-angle spinning (MAS) techniques, on a series of heat-treated silica gels that were silylated by hexamethyl-disilizane (HMDS). This was an attempt to elucidate details of the surface OH population of unsilylated samples. They observed that the complete removal of all silanol groups from silica is probably approached only at temperatures >1000 °C. Their studies showed that ^{29}Si NMR methods can be used to measure surface OH concentrations or bulk OH densities with good precision and accuracy for silica gel samples that are preheated over a wide range of temperatures. Measurements are not complicated by the presence of molecular water and therefore do not require the preparation of completely anhydrous samples. Further NMR studies favored the linear growth model for gel formation[112] compared to the cyclic oligomers.

Vacuum- and air-dried gels studied by ESR after γ-radiation[113,114] and X-ray exposure[115] revealed that low-temperature annealed gels showed the presence of organic free radicals, e.g., CH_3 and C_2H_5, whereas after high-temperature annealing only the O_2^- radicals were detected. NMR and Raman spectroscopy was used to study the sol–gel process for TMOS. The addition of formamide hinders the hydrolysis, in part, by increasing the viscosity of the solution and thereby increasing the proportion of bulky dimers, which are slower to hydrolyze. Also, the strong hydrogen bonding of formamide with Si–OH and CH_3–OH bonds tends to slow hydrolysis.[116] The use of drying control chemical additives (DCCA) to affect gels in the formation stage and drying state was reviewed.[117] It was shown that formamide decreases the hydrolysis rate sixfold but increases the polymerization rate slightly.

The influence of DCCA on the different steps of the sol–gel–glass formation was characterized by ^1H NMR in liquid and the solid state using a combination of multiple-pulse and magic-angle spinning methods.[118] The appearance of NH_4^+ ion together with formic acid under strongly acidic conditions was confirmed. Heat treatment of the gels at 60 °C led to the disappearance of alkoxy groups after some days.

DCCAs (e.g., formamide, glycerol, and oxalic acid) control the rate of hydrolysis, the rate of condensation, the pore size distribution, and the pore liquid–vapor pressure, which in turn improves the strength of the gel, making it better withstand the capillary stress. Adachi et al.[119] reported better results in drying gels by using dimethylformamide. Mizuno et al.[120] developed a new technique to avoid cracks during drying of gels by increasing the hydroxy groups in the gel. The substitution of residual alkoxy groups by OH groups was made by immersing the gels into a solution of high water content. By this method the gel could be dried very quickly without any special care to maintain the shape. The drying rate was about 5 times faster than for nontreated gels. The microstructure of the gels could also be controlled by changing the treating solution.

Drying behavior of lithium aluminum silicate prepared from hydrolysis of methanolic solutions of lithium and aluminum nitrates was studied during low-tem-

perature natural evaporation.[121] The total drying shrinkage though independent of the drying rate was anisotropic with respect to the radial and axial dimensions. The importance of cross-linking in strengthening the gels was emphasized.

Yoldas studied the hydrolytic and condensation process of TEOS[122,123] using NMR and size exclusion chromatography (SEC). In general, it was concluded that higher concentrations of SiO_2 result in a higher number of bridging oxygens (higher degree of polymerization). The hydrolysis of TEOS was compared with $CH_3Si(OC_2H_5)_3$ (MTES) and $(CH_3)_2Si(OC_2H_5)_2$ (DMDES).[124] Gel formation did not occur with DMDES where phase separation was noted. Viscosity and IR measurements showed TEOS and MTES to be similar in hydrolysis and polymerization.

Light scattering of silica sols was shown to validate the application of SEC.[125] The gel formation from various alkoxides was studied, and air-drying was compared at room temperature and elevated temperature.[126] The various stages of the sol–gel process were followed by viscosity, IR, TGA, DTA, and BET measurements.[127]

There does not seem to be any report on an attempt to freeze-dry the alcogel. The freeze-drying of cellulose gels has been studied extensively,[128] and an apparatus is described by which the water can be continuously removed from a sample and replaced by ethanol. Freeze-dried cellulose acetate[129] was characterized by a porous structure that is useful for the separation of gases. There does not appear to be anything intrinsically wrong with the idea of freeze-drying the alcogel, and this belief has been confirmed.[130] A properly cross-linked transparent alcogel that is thoroughly exchanged with a high-melting-point solvent should dry at ambient temperature and pressure without cracking or becoming opaque. This has yet to be verified. Such experiments are in progress in the authors' laboratory, and results have been encouraging—transparent xerogels with porosity of about 70% have so far been produced.

V. Applications

A. High-Energy Physics

The need for a low-density material with good optical quality for use in Cerenkov counters played a historical role in the development of high-quality, transparent aerogels. Cerenkov counters require a material with an index of refraction between 1.0 and 1.3. Detectors were previously made with pressurized gas and required solid walls and heavy construction. Aerogel detectors can be easily constructed with an index of refraction between 1.007 and 1.24, are extremely light, and are of simpler construction. Aerogel Cerenkov detectors[131] have been in use since the early seventies in accelerators at CERN and Berkeley and were recently used in space astrophysics by NASA.[132]

B. Superinsulation and Aerogels in Luminescent Solar Concentrators

i. Superinsulation: Thermal Properties and Energy Conservation

Because of their extremely low thermal conductivities, low densities, and high porosity, an ideal applica-

TABLE IV

(a) Steady-State Thermal Conductivities[a]

run	remarks	T_h, °C	T_c, °C	k, BTU h⁻¹ ft⁻¹ °F⁻¹	k, W/(m K)	k_{av}, BTU h⁻¹ ft⁻¹ °F⁻¹
1a	expt 1 (6/80)	98.0	19.7	0.0275	0.0476	0.0301
1b	ρ = 0.119 g/cm³	98.7	20.0	0.0308	0.0533	
	Δx = 10.05 mm					
1c	A = 25.83 cm²	98.6	21.8	0.0321	0.0556	
2a	expt 2 (6/81)	88.8	35.6	0.0580	0.1004	0.0454
2b	ρ = 0.14 g/cm³	94.5	37.8	0.0250	0.0433	
	Δx = 8.05 mm					
2c	A = 25.02 cm²	92.8	37.9	0.0533	0.0922	

(b) Non-Steady-State Thermal Conductivities[a,b]

run	time, s	T_{h1}, °F	T_{h2}, °F	T_{mid}, °F	k, BTU h⁻¹ ft⁻¹ °F⁻¹
1	0.0	83.2	83.5	83.2	
	83	139	134	123	0.0043
	173	142	146	139	0.0041
	263	147	144	143	0.0041
2	0.0	82	84	82	
	32	110	123	105	0.0040
	122	147	143	136	0.0045
	212	150	150	147.5	0.0052

(c) Results of the Aerogel Window Steady-State Thermal Testing[a,c]

run	internal press., mmHg	T_{hb}, °F	T_{cb}, °F	T_{h1}, °F	T_{c4}, °F	mass of cold air, lb mol h⁻¹	aerogel k, BTU h⁻¹ ft⁻¹ °F⁻¹	window U_0, BTU h⁻¹ ft⁻² °F⁻¹	R factor, h ft² °F BTU⁻¹
1	744	171	118	106	86.0	2.154 × 10⁻³	8.86 × 10⁻⁴	0.0275	36.4
2	743	171	112	108	86.0	2.006 × 10⁻³	7.30 × 10⁻⁴	0.0217	46.0
							8.08 × 10⁻⁴ [d]	0.0246[d]	40.6[d]
3	600	172	114	109	86.9	1.593 × 10⁻³	4.63 × 10⁻⁴	0.0144	69.5
4	596	172	111	110	85.5	1.534 × 10⁻³	3.93 × 10⁻⁴	0.0128	77.8
							4.28 × 10⁻⁴ [d]	0.0136[d]	73.5[d]

[a] Reference 5. [b] k_1(av) = 0.0041; k_2(av) = 0.0045. [c] T_{hb} = well-mixed temperature of hot-side air; T_{cb} = well-mixed temperature of cold-side air; T_{h1} = thermocouple temperature of hot glass surface; T_{c4} = thermocouple temperature of cold glass surface. [d] Average values.

TABLE V

(a) Literature Values of the Thermal Conductivity[a]

powder	remarks	density, lb ft⁻³	gas press., mmHg	interstitial gas	conductivity,[b] BTU h⁻¹ ft⁻¹ °F⁻¹	conductivity, W m⁻¹ K⁻¹
silica aerogel	chemically prepared (250 Å)	6.2	10⁻⁴		12 × 10⁻⁴	21 × 10⁻⁴
		6.2	628[c]	N_2	113 × 10⁻⁴	196 × 10⁻⁴
		6.2	628	He	358 × 10⁻⁴	620 × 10⁻⁴
		6.2	628	H_2	462 × 10⁻⁴	800 × 10⁻⁴

(b) Literature Conductivities[d]

air		CO_2		CCl_2F_2	
press., mm	conductivity[e] × 10⁵	press., mm	conductivity[a] × 10⁵	press., mm	conductivity[e] × 10⁵
740	4.85	745	4.33	740	3.71
387	4.06	397	3.87	406	3.38
206	3.61	206	3.42	259	3.18
183	3.63	100	3.06	123	2.86
94	3.26	49	2.98	59	2.63

[a] References 5 and 265. [b] 1-in. sample thickness, boundary temperature of 804 and −323 °F. [c] Barometric pressure at Boulder, CO. [d] References 5 and 137. [e] Conductivities in cal cm⁻¹ s⁻¹.

tion of aerogels is as a superinsulating window spacer with an extremely low loss coefficient of about 0.5 W m⁻² K⁻¹. In his pioneering work, Kistler demonstrated that the thermal conductivity of aerogel cakes is of the order of 0.02 W m⁻¹ K⁻¹ at ambient pressure in air and 0.01 W m⁻¹ K⁻¹ if evacuated. Considering the high transparencies obtainable with aerogel, it is apparent that it has a vast potential for the reduction of heat losses in all kinds of window systems.

As indicated earlier, the implication of aerogels for superinsulated windows is a recent development.[2] However, the subject has been patented in France by Zarzycki et al.[133] and in the U.S.A. by Hunt and Tewari.[85b] Thus, it would appear that besides the Berkeley group and the Swedish group, there is a French group also involved in insulated windows. The results from

the Berkeley group were recently reviewed by Hunt.[134,135]

The first direct application of silica aerogels for transparent insulated windows was recorded by Schmitt and Greiger-Block.[136] Schmitt used ethyl orthosilicate instead of methyl orthosilicate because of the higher toxicity of the methyl ester. Hydrolysis was performed with either hydrofluoric or hydrochloric acid. Because of the difficulty in handling the large pieces of aerogel, the hydrolysis and setting of the alcogel were made directly between two plates of glass. Samples with porosities of 0.93–0.97 were recorded, with optical properties shown in Figure 9.[4] The results of some thermal conductivity measurements are given in Table IV. Previously determined literature values are shown in Table V. The values that have been used[2] are about
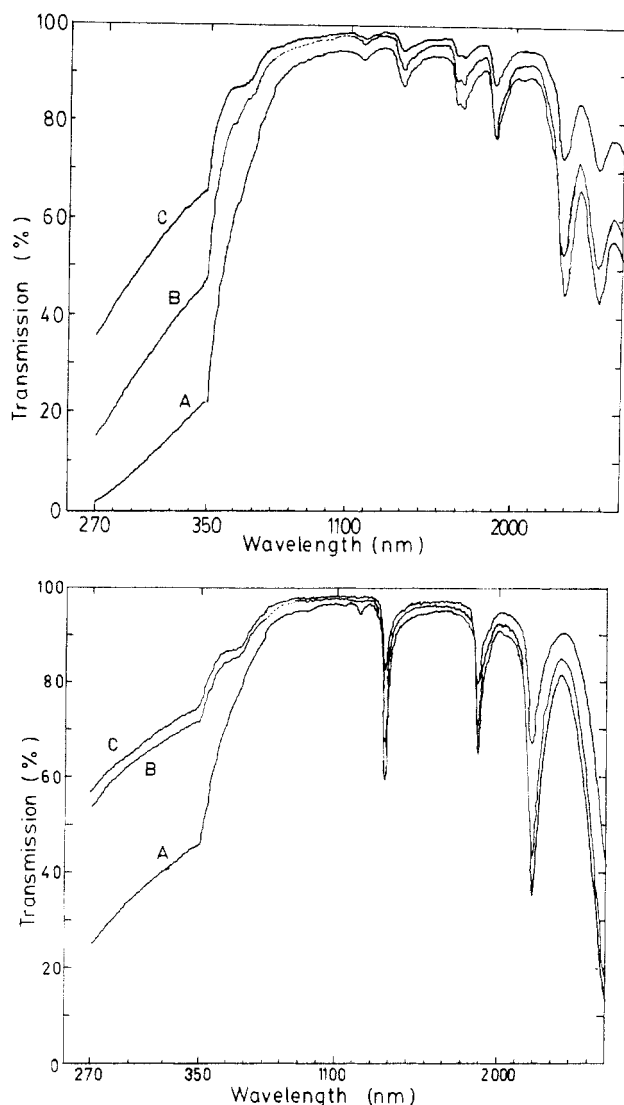
Figure 9. (a) Visible transmission spectra of untreated aerogel samples of thickness 8.36 (20A1), 4.27 (20A2), and 2.04 mm (20A3). (b) Visible transmission spectra of heat-treated (300 °C) and desiccated aerogel samples of thickness 8.36 (20A1), 4.27 (20A2), and 2.04 mm (20A3). Reprinted with permission from ref 5; copyright 1982 University of Wisconsin, Madison.

0.02 W m^{-1} K^{-1}. This can be reduced to half by the use of other filling vapors such as CCl$_2$F$_2$.[137-139]

Infrared heat transfer in transparent aerogel was investigated by Fricke[140] and Caps and Fricke.[141] They have reported values for radiative conductivity of an evacuated double-pane window with a silica aerogel spacer to be below 0.002 W m^{-1} K^{-1}. They estimated the total thermal conductivity of aerogel to be on the order of 0.007 W m^{-1} K^{-1}, which corresponds to a total loss coefficient, U, of 0.7 W m^{-2} K^{-1} for a 1-cm-thick aerogel tile. Thermal and solar optical properties of silica aerogel for use in superinsulating windows have also been investigated by Hartmann et al.[142] at Berkeley. They report that radiation heat transfer through aerogel is not a significant problem in the temperature range relevant to insulating windows. The thermal performance of an aerogel can be improved by replacing the pore gas with one of lower conductivity or by evacuating the aerogel to pressures below 0.1 atm. For a gap spacing of 12.5 mm, evacuated aerogel windows have a calculated U value of about 0.5 W m^{-2} K^{-1}.

Goetzberger et al.[143] reported that using aerogel as insulation for passive solar energy applications in buildings resulted in as much as 50% and 90% reductions for heat energy demand in three winter months in Freiburg. Another positive aspect of aerogel insulation is that it is nonflammable. Indirectly, as a result of the energy saving from aerogel insulation, adverse environmental consequences of present heating technology used in buildings would also be reduced.

Fricke et al.[144] investigated the thermal loss coefficients of monolithic and granular aerogels used as superinsulating spacers under evacuation and reported these to be around 0.5 W m^{-2} K^{-1} for layers about 15 mm thick. Parameters such as radiative temperature, sample density, boundary emissivity, and internal gas pressures were considered. Applications and benefits of thermal superinsulation were considered. Applications and benefits of thermal superinsulation with aerogels include the following: (i) the efficiency of hot-water storage systems could be improved; (ii) electric house heating/storage systems could be made smaller due to smaller losses; (iii) superinsulated steam heating systems and steam pipes with smaller diameters than conventional ones could be used; (iv) new high-temperature batteries, such as sodium sulfide batteries for electric vehicles, which depend on load-bearing superinsulations to keep the reactants liquid during parking periods could be developed; (v) superinsulated refrigerators and freezers could be built with less cooling power and larger useful volume for a given outer geometry than conventional systems; (vi) greenhouses could be built to be more energy efficient; (vii) solar ponds for collection and long-term storage of solar energy could be built.

Nilsson et al.[145] investigated the thermal conductivity λ and the specific heat capacity ρc_p of aerogel as a function of temperature. They also considered the volume dependence of thermal conductivity from the viewpoint of window insulation using blocks of aerogel of dimensions as large as $190 \times 190 \times 32$ mm. The thermal conductivities at atmospheric pressure and normal outdoor temperatures (-20 to $+50$ °C) for two samples with an initial density of 109 g/L were determined. The thermal conductivity at room temperature was found to be 0.0131 W m^{-1} K^{-1} and increased linearly with temperature up to 40 °C, where there was a sudden change of slope. At a temperature of 50 °C, λ reached a value of 0.0178 W m^{-1} K^{-1}. As the temperature was lowered, λ decreased with a slope of only 35×10^{-6} W m^{-1} K^{-2}, giving a great hysteresis to the λ-T curve; however, there was no hysteresis effect noticed when the temperature was lowered to -20 °C and then raised to room temperature—the value of λ after this cycle was 0.0167 W m^{-1} K^{-1}. The second example, taken up to 100 °C and then back to room temperature, showed similar behavior. The variation of heat capacity per unit volume, ρc_p, with temperature was also studied, and the quoted value at room temperature was 0.24 MJ m^{-3} K^{-1}, with a corresponding c_p value of 2.2 J g^{-1} K^{-1}. A variation of 25% °C^{-1} was reported for c_p. Comparison with compressed material (up to 0.4 GPa) revealed no pronounced difference in the c_p vs T curves, except that at the highest temperature (200 °C) the uncompressed material showed up to 5% higher values for c_p. Variation of λ and ρc_p with pressure showed no

marked changes in either quantity up to 25 MPa. A marked change occurred at that pressure; the change was time dependent, indicating that it may be due to volume relaxation.

Platzer et al.[146] investigated the solar transmission of aerogel pellets of 0.5–8.0-mm diameter produced by BASF Ludwigshafen that were used as fillers in windows under different outdoor conditions. Because of the scattering of blue light, the outdoor transmittance varied depending on weather conditions. Transmittance values ranging from 64 to 70% for 1 cm of filling thickness were reported. A simple theoretical model was developed to calculate mean solar transmittance for aerogel layers, including a correction factor for scattering and absorption.

Schreiber et al.[147] reported on the potential of aerogel as a transparent insulation material for buildings from an engineering viewpoint. A comparison of various insulating materials used in buildings was made, with reference to Copenhagen weather conditions and different wall constructions; the U values for lightweight wall constructions were 0.27 (insulated) and 0.81 W m^{-2} K^{-1} (uninsulated). On the basis of a model calculation, it was reported that an estimated 350 kWh m^{-2} of heating energy could be saved per year by insulating high-mass wall constructions with aerogel whereas for a lightweight type of wall, a saving of 50 kWh m^{-2} per year would still be possible. Considering the given boundary conditions, the comparison of an equivalent opaque insulation to transparent insulation would yield a yearly specific energy conservation of 30–100 kWh m^{-2} for the transparent insulation, depending on the orientation and type of the wall material.

ii. Aerogels in Luminescent Solar Concentrators

Another important use of aerogels is the luminescent solar concentrators (LSC). A luminescent solar concentrator is a planar layer of materials, usually contained on or in a transparent matrix of plastic.[148] The matrix is usually doped with an organic dye that fluoresces under incident solar radiation. If the refractive index of the matrix is sufficiently dissimilar from that of air, the fluorescent radiation is reflected and confined within the matrix and is ultimately directed to the outer edges of the plane where solar cells for energy conversion are placed. This subject has been reviewed by Reisfeld and Jorgensen.[149,150] Aerogel can be used as a material for flatbed solar concentrators when it is suitably doped with either organic or inorganic luminescent material such as dyes or rare-earth salts and made continuous by filling the doped aerogel with a monomer such as methyl methacrylate. Folcher et al.[151] have described LSC containing uranyl-doped glass and obtained quantum yields of 0.6–0.7 with low uranyl concentration (<1%). Avnir et al.[152] reported their work on Rhodamine 6G embedded in porous silica gel glass prepared from TMOS and discussed the advantages of inorganic oxide glasses as carriers of organic dyes. These advantages included photostability and thermal stability of the glass matrix; trapping of the dye molecule and its total isolation from undesired interaction with the neighboring dye molecules, impurities, and photodecomposition products; nonleachability of the dye; the ability to reach stable, yet very high dye concentrations; reduction of translational, rotational, and vibrational degrees of freedom of the trapped dye; and good transparency down to the UV region. Reisfeld[150] in another review discussed the fluorescence and nonradiative relaxations of rare earths in amorphous and on highly porous materials such as porous Vycor glass as well as applications of the rare earths Nd^{3+} and Ho^{3+} in combination with UO$_2$$^{2+}$ in luminescent solar concentrators.[151,152]

C. Sol–Gel Route to Glass Manufacture: Films, Fibers, Coatings, and Ceramics

Aerogels have also been used as a means of preparing low-temperature glasses. Such work generally consists of incorporating various different metal oxides within the gel to give rise to blends of silica glass.[153–157] A recent review of this topic was presented by Mukherjee.[158] It is interesting to note that the conversion of the gel to glass does not involve the removal of solvent by an autoclave at supercritical conditions. Numerous examples of such low-temperature glasses have been described.[159–167] The papers of a symposium, "Glasses and Glass Ceramics from Gels" (July 1983), have been published.[168–194]

Since the purpose of all of these papers was to prepare a low-temperature glass, the object of the process was to obtain a gel of high density. Gels of low density (0.60 g/mL) were reported[173] when drying was slow, but no mention was made of the transparency of the aerogels formed.

Though most of the symposium papers presented methods for the preparation of a pure or mixed gel, the control of viscosity was used[177] to reproduce pour conditions. Shrinkage was found to be greater when drying was conducted at higher temperatures.[178] Yoldas[180] discussed the factors affecting gel formation and structure, the important ones being the selection of starting compounds and host medium, water/alkoxide ratio, molecular separation by dilution, catalytic effects, reaction temperature, order of reactions in multicomponent systems, and aging and heat treatment, which involve time, temperature, and atmosphere. The influence of these factors was discussed with respect to gel formation involving Si(OC$_2$H$_5$)$_4$, B(OCH$_3$)$_3$, and Al(OC$_4$H$_9$)$_3$.

Congshen et al.[177] discussed the formation of ZrO$_2$–TiO$_2$–SiO$_2$ glasses by the sol–gel method. These glasses have low thermal expansion and are resistant to alkali corrosion, but it is difficult to prepare them by the conventional melting method because of their extraordinarily high melting temperatures (ZrO$_2$, ~2700 °C; TiO$_2$, ~1850 °C; SiO$_2$, 1713 °C). They synthesized these glasses by the sol–gel route using Zr(NO$_3$)$_4$·5H$_2$O, Si(OC$_2$H$_5$)$_4$, and Ti(C$_4$H$_9$)$_4$, and the resultant glasses contained 20 mol % TiO$_2$ and up to 30 mol % ZrO$_2$. Their detailed studies of hydrolysis, polymerization, gelation, and conversion of gel to glass made use of IR spectroscopy, DTA, and XRD. The viscosity evolution of the reaction system showed that environmental humidity and the catalyst used were important factors in the gelling process. During heat treatment, the color of the gel changed gradually, and DTA results indicated that the conversion of gel to glass would be complete at 650 °C. From XRD and IR data they concluded that Ti^{4+} act as network formers, while Zr^{4+} act as network modifiers. The formation of gels from colloidal SiO$_2$

particles was also reported.[181-184] Gels prepared for spinning fibers have been described.[186] In most cases, densification of the gel is encouraged, since the end use is a solid glass.[187] Thin coatings and plates[188] invariably broke into fragments on drying. The short review by Dislich[189] clearly illustrates the scope of the sol–gel technique. The remaining symposium papers (ref 190–194) discuss special applications of the process.

Schlichting[183] discussed oxygen transport through glass layers formed by a gel process. Oxygen diffusion rates for binary B_2O_3/SiO_2, GeO_2/SiO_2, Al_2O_3/SiO_2, and TiO_2/SiO_2 glasses were determined. To this end, silicon single-crystal material was coated with the appropriate glasses obtained from gel solutions by a dipping process and was subsequently heat treated. Schlichting pointed out that while it is difficult to prepare two-component glasses by a melting process, it is easy to prepare thin glass films of every composition, mostly on glass plates, by a gel process.

Segal[184] made a comparative study of two sol–gel routes used to form oxide ceramics, the first using colloidal dispersions and the second using metal alkoxide precursors. Methods of making shaped products such as spheres were described with the range of oxides that have been produced by sol–gel routes. The sol–gel route involving metal alkoxide is ideally suited for the preparation of small quantities of high-purity materials. The sol–gel processes that employ dispersible oxides can be used for large-scale production since they offer advantages for materials and energy economy.

Pentinghaus[185] discussed the use of alkoxide-derived gels as starting materials in experimental petrology and solid-state chemistry. Amorphous and homogeneous solids of many compositions can be prepared from alkoxide solutions via complexing, hydrolysis, and polycondensation followed by a final heat treatment. Many alkoxides of Na, K, Cs, Si, Ge, Be, and Al were used in his studies.

Jones et al.[186] described their studies on the use of technical ethyl silicate for preparing glass-like materials and fibers. Technical grade ethyl silicate was hydrolyzed by using tetravalent organotin compounds as catalysts for neutral hydrolysis and gelation. Transparent, glass-like gels can be formed, particularly if the water content is >16%. Systems with a water content between 8 and 16% show good fiber-forming ability, dibutyltin diacetate being the preferred catalyst. These systems show better fiber-forming ability than do similar systems using tetraethoxysilane. Viscosity measurements suggest that this is because the technical ethyl silicate contains a mixture of linear polysilicate oligomers.

Glaser et al.[187] discussed their work on the effect of the variation of $H_2O/TEOS$ ratio on the preparation and nitridation of silica sol–gel films. These films have many potential applications, particularly as scratch-resistant coatings, dielectric films, and oxidation or diffusion barriers. The film properties can be greatly enhanced by incorporation of nitrogen. Nitridation reactions provide a means for probing the surface chemistry and micromorphology of sol–gel films. Silica sol–gel films were deposited on silicon wafers by spinning solutions of varying $H_2O/TEOS$ ratio. The density of initial microporous dried gel films increased with $H_2O/TEOS$ ratio, and the amount of film shrinkage

observed during thermal treatment in N_2 or NH_3 decreased with increasing $H_2O/TEOS$ ratio. This is contrary to the behavior of bulk gels derived from solutions of increasing $H_2O/TEOS$ ratio. The trend is attributed to the fact that in films polymerization of the structure occurs in the absence of a liquid phase. Enhanced incorporation of nitrogen was observed during ammonia treatment of the films prepared with solutions of increasing $H_2O/TEOS$ ratio. Nitrided films showed signs of limiting the oxidation of the silicon wafers.

Sakka et al.[188] discussed the formation of thin sheets and coating films from alkoxide solutions. Thin-sheet formation is only possible with the starting solutions that exhibit spinnability in the course of hydrolysis and polymerization of the metal alkoxide. Thin-sheet formation becomes possible when the solution reaches viscosities ranging from 10 to 100 P and is possible from solutions with $H_2O/TEOS = 1.5-4$. The gel sheet becomes a transparent silica glass sheet, 10–40 μm thick, on heating to 800–1200 °C. Three methods were employed for thin-sheet formation. The first involved putting a wire ring into the solution and pulling it up so that the sheet formed on the ring. For the second method, the viscous alkoxide solution was drawn into sheets by passing through a slit. In the third method, the viscous solution was applied onto a nonadhesive plastic plate and removed after solidification. Coating films were applied to the substrate by the dip-withdrawal method. The films were then heated to convert the gel film to glass or ceramics. SiO_2, $BaTiO_3$, and transition-metal oxide–SiO_2 coating films were prepared, and transmittance characteristics were reported.

Dislich[189] reviewed the scope of the sol–gel processes and pointed out that for economical reasons, the sol–gel products must have special uses or process advantages. He noted the most interesting fields to be preforms for communication fibers, technical fibers drawn from solutions, unsupported films, hollow spheres for nuclear fuels, catalytic effects, and coatings. Coatings are the oldest sol–gel products, which have gained new impetus from multicomponent oxide syntheses. In this field, heat mirror coatings such as indium–tin–oxide (ITO) on float glass, necessary for energy-saving windows, are of greatest interest. Ideal requirements for products and processes involved in the development of coatings were discussed.

Arfsten[190] discussed applications of sol–gel-derived transparent IR-reflecting ITO semiconductor coatings. ITO film reflects long-wave IR radiation and thereby suppresses heat transport by radiation exchange. These films are highly transparent for solar radiation, and therefore windows composed of ITO-coated glasses are good passive solar collectors. A dip-coating process for sol–gel-derived ITO layers was developed, and the characteristics of such ITO coatings were described. Transmittance as high as 83% in the visible region, radiant transmittance of 66%, and total energy transmittance of 74% were reported.

Geotti-Bianchini et al.[191] described the preparation and characterization of Fe, Cr, and Co oxide films on flat glass from gels. One-component and multicomponent coatings were obtained on soda lime glass, their oxide content was determined, and their transmittance and reflectance were measured in the 300–2300-nm

range. The sun-shielding performance of these coatings was less than commercial sun-shielding glass.

Kaiser and Schmidt[192] reported that siliceous membranes can be reacted onto the surface of porous supports using the sol–gel method. Of the various possible techniques, reaction via the vapor phase is the most useful. A belt of filter media could be coated continuously and homogeneously using laboratory-scale equipment; the coated filter media showed improved cleaning behavior compared to uncoated samples.

Carturan[193] discussed the preparation of supports for catalysis by the sol–gel route. The surface area and thermal stability of $SiO_2/Al_2O_3/Na_2O$ supports prepared from alkoxides were studied as a function of time and temperature. The results indicated substantial stability in time at temperatures ≤ 250 °C, while progressive decrease in porosity was observed at higher temperatures. New supports were prepared by coating glass microspheres with layers of porous oxides such as Al_2O_3, TiO_2, ZrO_2, MgO, SiO_2, and Fe_2O_3. Formation of the porous layer was achieved by extending the gel method to the coating technique. BET surface area, electron microscopy results, and other features relevant to these systems were discussed. The data suggests that these materials may be exploited as effective supports for metallic catalysts.

Philip and Schmidt[194] discussed methods of synthesizing materials for hard contact lenses from an epoxide-substituted Si and Ti alkoxide, using the sol–gel process. To obtain sufficient tensile strength, polymethacrylates were incorporated as linear cross-linking elements, using a methacryloxy-substituted alkoxysilane as a hook between the siliceous network and the polymer chain. The incorporation of titania led to dense monolithic products that could be cured with only minor shrinkages. Good wettabilities (contact angle with water, $25 \pm 5°$) are due to glycol groupings formed by epoxide radicals. O_2 permeabilities of $P = (13 \pm 1) \times 10^{-11}$ mL of O_2 cm^2 mL^{-1} s^{-1} mmHg^{-1} result from the silicone-like OSiR structure elements, where R denotes a silicon–carbon-bound organofunctional radical. The corresponding values for silicone rubber, another material used for contact lenses, are as follows: contact angle with water, 85–100°; $P = 70 \times 10^{-11}$ mL of O_2 cm^2 mL^{-1} s^{-1} mmHg^{-1}. Though silicone rubber has a very good oxygen permeability, it is very hydrophobic. Thus the Si and Ti glasses prepared by the sol–gel process have an advantage.

Mulder et al.[195] discussed the preparation, densification, and characterization of autoclave-dried silica gels. A two-step hydrolysis process was followed. First, tetraethoxysilane dissolved in ethanol was partly hydrolyzed at 50 °C with acidified water. Then polymerization was achieved by adding alkaline water at room temperature; the gelling time is dependent on the proportion of acid and base solutions added and can be reduced to a few minutes by the addition of the alkaline solutions. Before gelling, the solution was poured into molds of the desired shape. The molds were coated with a two-component silicone rubber, which serves as an antiadhesive layer. The gel was dried in an autoclave in the presence of an inert gas (N_2) and at supercritical conditions (300 °C, 8 MPa). Extremely low density gels were obtained by using extremely dilute solutions. Very low densities of 0.03 g/mL and a specific surface area

TABLE VI[a]

(a) Experimental Data on the Densification of SiO_2 Gels

gel	temp, °C	gel density, g cm^3	spec surf area, m^2/g	particle diam,[b] nm
1	300	0.16	740	8
2	800	0.16	780	8
3	1150	0.27	530	11
4	1200	0.66	160	12
5	1210	1.00	76	24
6	1225	1.41	36	40
7	1250	2.08		

(b) Initial N_2 Pressure and Corresponding Density and Shrinkage of a Gel

N_2 press., bar	spec density, g/cm^3	shrinkage, %
0	0.49	73 (cracked)
10	0.27	52
40	0.14	7
80	0.13	0

Experimental Data on Low-Density Gels

gel	gel density, g/cm^3	particle diam,[b] nm	spec surf area, m^2/g	sphere density,[c] g/cm^3
1	0.15	20	520	0.38
2	0.05	10	1080	0.37
3	0.03	8	1590	0.31

[a] Reference 195. [b] Approximate diameter of the particles as derived from the TEM pictures. [c] Calculated from the specific surface area and particle diameter measurements, taking into account the degree of interconnection of the particles.

as high as 1600 m^2/g were achieved (Table VI). TEM studies characterized the structure of the gels as a highly branched network of SiO_2 spheroids of diameter <20 nm. A TEM study of the densification of low-density gels to glass revealed that during heating, spherical particles of porous material coalesce into larger spherical particles of SiO_2, while the interconnected structure of the gel remained unbroken. The structure began to show serious alterations only after 800 °C. At 1250 °C the densification was almost complete in 12 min as a consequence of polymerization by the continued dehydration.

Achtsnit[196] described the development of microporous silica fibers from sodium silicate. By chemical and physical modification of a commercial product, a spinnable high-viscosity dough was obtained. Sodium silicate fibers are the intermediate product; as a result of a cation exchange, the hydrolysis-sensitive fibers were converted into silica fibers in an acid bath, and subsequent washing with water yielded a silicon dioxide content above 99.6%. The physical properties, particularly porosity and tensile strength, can be influenced in the final drying process. These low-density fibers (1.5–2 g/mL) are the lightest inorganic fibers available and they have a low thermal expansion coefficient, good thermal stability up to 1100 °C, and a low dielectric constant (<4 at 1 MHz). Because of their low thermal conductivity, they could also be used in thermoelectric insulation sectors.

Pettit and Brinker[197] discussed the use of the sol–gel method for producing thin films for solar energy applications. Thin films were formed by depositing the alcohol/water solution of alkoxides of Si, B, or Al on a substrate by spinning, dipping, or spraying. On heating the film to moderate temperatures, 400–500 °C, dense glass films or stable porous films were produced. The main aspects of solar energy applications discussed were as follows: (i) encapsulation of black chrome so-

lar-selective coatings improved the high-temperature thermal stability by a factor of 2.7; (ii) formation of porous, antireflective coatings on glass envelopes used in solar thermal collectors increased the solar transmittance of the glass from 0.91 to >0.96; (iii) double-layer, antireflective coatings of SiO_2-TiO_2 on silicon solar cells reduced their solar reflectance from 0.36 to 0.04 and thereby improved cell efficiencies by ~50%; (iv) protective coatings applied to silvered stainless steel substrates were used to form structural solar mirrors. Averaged solar specular reflectance values of 0.90–0.91 were obtained.

Avnir[198] et al. utilized the sol–gel process to incorporate several organic dyes, including Rhodamine 6G, in inorganic oxide thin films. Fluorescent thin films were prepared by this low-temperature sol–gel process with the aid of a surface-active agent with good homogeneity and reproducibility. A variety of fluorescent molecules were embedded in either silica or silica-titania films. The dye molecules were not leached out by water. Absorption and emission spectra, enhanced photostability, longer lifetimes, and energy transfers between trapped dye molecules were described and discussed in terms of the effects of molecule matrix isolation on these properties.

Gel formation in alumina and silica from the alkoxides has been studied by Yoldas.[199] The Raman and IR spectra changed in a gel when heated from 40 to 500 °C and was used to follow the process of glass formation in TEOS to SiO_2.[200]

Mixed-oxide gels of TiO_2-SiO_2 were prepared by Yamane et al.[201] by using a bulky alkoxide for Ti(OR)$_4$ and a methoxide for Si(OR)$_4$. Several methods were compared, but the work only considered the homogeneity of the glass. A similar study was reported by Gonzalez-Oliver.[202] The gels were dried first at room temperature and then in a ventilated oven at 50–60 °C for 3–4 weeks. The gels obtained were hard, clear, and crack-free. However, no density values were given. Similar mixed glasses of SiO_2-TiO_2 were prepared by Hayashi et al.[203] by the alkoxide–gel process. The drying process for the gels took 3 months. Though transparent glass was formed at 800 °C no mention was made of the properties of the gel. Some recent work reported[204] on silica–alumina gels that have been made from the silicon alkoxide hydrolyzed with Al(NO$_3$)$_3$ in alcohol. However, the gels were ground to a powder before being fired at high temperature. A gel from NaOCH$_3$ and B(OBu)$_3$ was reported to fuse at 500 °C to full densification and to resemble the melt-quenched glass.[205] Drying of the gel took several days as the temperature was raised from 25 to 500 °C.

An interesting review of the applications of sol–gel glasses has been given by Dislich.[206] Though numerous applications are described, the insulating properties of the aerogel were omitted.

Gel formation starting with pyrogenic silica was described in terms of the characteristics of the starting silica.[207] DTA and NMR were used to determine the extent of bound water. Ultrasonication of the aqueous dispersions tended to break up the clusters.[208] The polymerization of siloxanes was reviewed[209] in relation to glass formation.

The structure of gels in relation to glass formation was described by Zarzycki.[210] Comparison was made between the open-pore and closed-pore models.

Raman studies were reported on TiO_2-SiO_2 glasses prepared by the sol–gel process.[211]

Wenzel[212,213] has summarized the role of the sol–gel process and its effect on the glass industry.

Gel formation from fumed silica in various organic solvents was studied primarily by TGA.[214] Several papers by Brinker and Scherer on the sol–gel–glass process have presented a good review of the process and its problems.[215–218] Potential application of the sol–gel process was detailed by Gottardi.[219]

Colored coatings were prepared by the sol–gel process by adding Co, Cr, Mn, Fe, and Cu to the gelling solution. Thin coatings of the gel were not colored sufficiently to have suitable applications.[220]

Gonzalez-Oliver et al.[221] described electroactive antimony-doped tin oxide coatings on display and borosilicate glasses. They were prepared by dip-coating and spraying techniques, starting from alkoxides in n-butyl alcohol or acetylacetone solvents containing small quantities of catalysts and water.

Electron micrographs of silica xerogels showed particle agglomeration during heating to form dense glass.[222] The effect of fluoride on gel formation and drying was studied, and it was determined that shrinkage decreases with the addition of fluoride.[223] Gels dried in an autoclave at supercritical conditions were shown to exhibit no shrinkage when the initial N$_2$ pressure in the autoclave was about 80 atm.[224]

A series of papers by Sherer[225–230] on gel formation and drying have clearly defined the problem and present some interesting solutions.

The physical and chemical processes occurring during the aging, drying, and sintering of inorganic gels were discussed in recent reviews.[231,232] Various advantages and disadvantages of the sol–gel process, the factors governing the structure and microstructure during gelation, and subsequent heating were discussed by Mackenzie.[233] Quinson et al.[234] have followed the drying evolution of wet silica gels prepared by esterification-controlled hydrolysis and reported the existence of both macropores and mesopores in wet gels. In the dry state, only the mesoporous structure could be studied. The observed behavior conformed to the Scherer model. The gel to glass process was reviewed by Dislich.[235] Other aspects of glass prepared by the sol–gel process have been outlined.[236–242]

Ulrich[243] reviewed the prospects of the sol–gel process in detail and emphasized the ultrastructural control of material achieved in glass, glass-ceramics through sol–gel processing. Examples of gel monoliths SiO_2-TiO_2, LiO_2-Al_2O_3-SiO_2-TiO_2, advanced molecular ceramics, molecular glass composites, and nonlinear optical sol–gel composites (CaZr$_{24}$P$_6$O$_{24}$) have been presented. A nanocomposite, Ca$_{0.5}$Sr$_{0.5}$Zr$_2$P$_6$O$_{24}$, prepared by the sol–gel route had zero thermal expansion within the 0–500 °C temperature range.

Krol et al.[244] used Raman spectroscopy to study the influence of gelling in an autoclave and drying with SOCl$_2$ or Cl$_2$ on the properties of monolithic silica gels, with emphasis on the surface and bulk OH content and densification behavior.

Suwa et al.[245] described the densification and sintering behavior of structurally diphasic Al$_2$O$_3$ and Al$_2$O$_3$-MgO xerogels. With isostructural seeding, they

were able to achieve enhanced densification as well as sintering at lower temperatures. Microstructural characterization by XRD showed uniform grain growth with little or no porosity.

Oda et al.[246] applied the sol–gel method to prepare ultrafine α-LiFe$_5$O$_8$ particles using alkoxide as the starting material.

Sun et al.[247] described the preparation of rare-earth silicate glasses by the sol–gel method starting with rare-earth carbonates of Pr, Dy, and Er and TEOS, and densifying the gel at 800 °C. Infrared and visible spectra and magnetic susceptibilities were reported.

Tanaka et al.[248] studied the mechanical instability of gels at the phase transition—when immersed in a liquid, gels undergo a volume phase transition, with the volume change at the transition as large as a factor of 1000. The physical basis underlying the formation and evolution of the pattern during swelling is discussed for an ionized acrylamide gel as an example. An ESR and ENDOR study of V$_2$O$_5$ gels was reported by Barboux et al.[249] They studied the swelling of the gel in water and showed that water molecules belong to the coordination polyhedron of V(IV) ions, giving rise to hydrated vanadyl species.

Bali et al.[250] studied the conduction mechanism in V$_2$O$_5$ xerogel films of thicknesses ranging from 5 to 1000 nm and showed that the conduction is purely electronic. Conductivities are 2 orders of magnitude higher than those of single-crystal V$_2$O$_5$ and 2 orders of magnitude lower than the V^{4+} concentration in either the films or the single crystals. Bali suggests that the higher conductivity of xerogels is associated with film hydration, which increases the number of V^{4+} sites active in the conduction process.

Calemczuk et al.[251] discussed specific heat and thermal conductivity measurements, performed in the temperature range 0.1–10 K, on low-density silica aerogels (0.27–0.87 g/mL) and commented on the unusual behavior compared with glasses. The results, together with sound velocity data, were interpreted within a fractal model of the structure.

The sol–gel process applied to the encapsulation of nuclear waste[252] was described. Plodinec[253] discussed the vitrification of nuclear waste and the problems to tackle in relation to glass technology for containment of 50–60 radioactive elements in a durable borosilicate glass.

The sol–gel method was used to prepare TiO$_2$ film on a nesa glass substrate. The sol was prepared by mixing Ti(O-i-C$_3$H$_7$)$_4$, anhydrous C$_2$H$_5$OH, and water. The film was obtained by dipping a nesa glass substrate in the TiO$_2$ sol and subsequently pulling it up at constant speed (0.15 mm s^{-1}). The resulting film was heat treated at 500 °C for 10 min. The above operation was repeated until a thick film of 2 μm was obtained. The dip-coating method makes it possible to obtain a large surface area of thin films, which might have great effects on the photoelectrochemical behavior of this semiconductor, which is used as a photoelectrode in solar energy conversion.[254,255]

The importance of the sol–gel method in making nuclear fuel pellets, low-temperature ceramic material such as ceramic fibers, thin coatings, and abrasive grain has been reviewed,[256a] with special emphasis on the increasing likelihood of developing electronic ceramic

materials. Although purity and control of the stoichiometry of these ceramics are essential, thin layers are adequate. Recently, the sol–gel process has also been applied to the preparation of high-temperature ceramic superconductors such as YBa$_2$CuO$_{6+x}$ (T_c = 91 K), La$_{1.9}$Ba$_{0.1}$CuO$_4$ (T_c = 23 K),[256b] and YBa$_2$Cu$_3$O$_x$ (T_c = 56 K).[256c]

D. Other Applications

i. Catalysis

Aerogels show great promise in catalytic applications. Teichner and co-workers detailed some recent applications of aerogels as catalysts. Compared to conventional catalysts, their activity and selectivity in various catalytic reactions appear to be much higher. Besides, in some catalytic reactions common catalysts become deactivated with time on stream.

Teichner[257] reported on the preparation of aerogels of inorganic oxides, pure as well as mixtures of two or more oxides. In the case of binary or ternary oxides, the less refractory ones such as NiO may be reduced to the metallic state, in which the metal particles are stabilized in the divided form by other oxide(s) like silica or alumina, which act as a support of the metal. Besides silica, other examples were Al$_2$O$_3$, ZrO$_2$, MgO, Fe$_3$O$_4$, TiO$_2$, Al$_2$O$_3$–MgO, TiO$_2$–MgO, and ZrO$_2$–MgO. Mixed-oxide aerogels that have good catalytic properties were cited as Al$_2$O$_3$–NiO, Al$_2$O$_3$–Cr$_2$O$_3$, SiO$_2$–NiO, and SiO$_2$–Fe$_3$O$_4$. Some examples of aerogel catalysts are described below.

TiO$_2$ Aerogels. TiO$_2$, in the form of anatase, exhibits a surface area of 120 m^2/g and is used at room temperature as a photocatalyst for partial oxidation of paraffins, olefins, and alcohols into ketones and aldehydes. In the case of paraffin-like isobutane, the conversion yield is higher on the TiO$_2$ aerogel than on other forms of anatase.

Gels have been used for stabilization of reactive free radicals. Gesser et al.[258] stabilized a high concentration of O$_2^-$ on the surface of amorphous TiO$_2$ gel, which was annealed at temperatures <550 °C. Ragai[259] reported on the production of trapped O$_2^-$ free radicals generated in a titania gel matrix by the initial reaction of Ti(III) ions with H$_2$O$_2$ and the subsequent precipitation with NH$_4$OH. The detected paramagnetic species could be complexes with Ti(IV) ions. The trapped O$_2^-$ free radicals had a high stability, extending as long as 2 years.

Fe$_2$O$_3$–SiO$_2$ and Fe$_2$O$_3$–Al$_2$O$_3$ Aerogels for Fischer–Tropsch Synthesis. These catalysts, which have surface areas on the order of 800 m^2/g, are important in view of their direct potential in alleviating the inevitable shortage of crude oil. Teichner et al.[260] reported that ferric oxide supported on silica or alumina aerogels shows a catalytic activity in the Fischer–Tropsch synthesis of hydrocarbons from catalytic hydrogenation of carbon monoxide that is 2–3 orders of magnitude higher than that of the commonly used reduced iron catalyst.
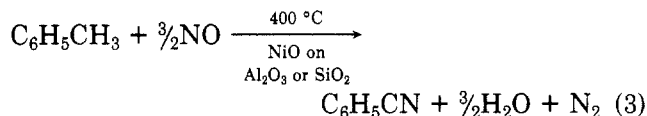
Ni–Al$_2$O$_3$ Aerogels. These catalysts were obtained by hydrogen reduction of NiO–Al$_2$O$_3$ aerogels.[260b] The good dispersion of nickel is preserved only when the stoichiometric amount of water is used in the hydrolysis of the starting organic derivatives. In the dealkylation of ethylbenzene into benzene, the aerogel catalysts show

limited selectivity (1%) toward the undesirable side reaction of the rupture of the aromatic ring.

Cu–Al₂O₃ Aerogels. These aerogels have been used in a fluidized bed reactor for selective hydrogenation of cyclopentadiene into cyclopentene with a selectivity of 100% at a reaction temperature of 180–220 °C.[260b] They are also 100% selective toward the partial hydrogenation of acetylene to ethylene.

NiO–Al₂O₃ Aerogels. NiO–Al₂O₃ aerogels are almost 100% selective toward partial oxidation of olefins.[259,260b] Isobutene is converted to methacrolein and acetone. NiO–Al₂O₃ aerogel is selective toward partial oxidation of propane (50%) and of isobutane (75%) to acetone. With ternary aerogels NiO–SiO₂–Al₂O₃ the selectivity may even be 100%.

Nitriles are intermediate monomers for plastic polymers like poly(acrylonitrile) and poly(methacrylonitrile). The usual method is based on the oxidation of olefins in the presence of oxygen and ammonia (ammoxidation) and of conventional catalysts containing oxides of Sn and Sb or of Mo and Bi. Paraffins and aromatics are not converted into nitriles by these catalysts. Teichner reported that by using NO in the presence of NiO–Al₂O₃ or Ni–SiO₂ aerogel at 440 °C, toluene and xylenes could be converted into the corresponding nitriles, propene into acrylonitrile, and isobutene and isobutane into methacrylonitrile (eq 3).

$$C_6H_5CH_3 + \tfrac{3}{2}NO \xrightarrow[\substack{\text{NiO on} \\ \text{Al}_2\text{O}_3 \text{ or SiO}_2}]{400\ °C}$$
$$C_6H_5CN + \tfrac{3}{2}H_2O + N_2 \quad (3)$$

The aerogel catalysts were prepared from a solution of nickel acetate and aluminum *sec*-butoxide that were both dissolved in methanol and hydrolyzed by the stoichiometric amount of water to yield the mixed alcogel. This alcogel was finally dried in an autoclave under hypercritical conditions with respect to methanol. Cr₂O₃–Al₂O₃ aerogels were equally effective.[260b]

Xylenes were also converted into nitriles with a PbO–Al₂O₃ aerogel catalyst.[260b] With o-xylene, the selectivity in o-tolunitrile is 75% and 20% in phthalonitrile. With p-xylene, the selectivity in dinitrile is 50% with the same catalyst at 460 °C, using a feed containing an excess of NO (P_{NO} = 30 Torr, P_{xylene} = 15 Torr, P_{He} = 715 Torr).

Pd–Al₂O₃ Aerogels. Armor[261] et al. reported the use of Pd–Al₂O₃ aerogel, which had large pore volumes (6.5 cm³ g⁻¹) and high surface areas (642 m² g⁻¹), in complete and selective hydrogenation of nitrobenzene to aniline. Yields >1000 mmol of aniline/mmol of Pd were observed. Because of their enormous pore volume, aerogels have further potential as catalysts in hydrodenitrogenation and hydrodesulfurization processes.

Wang et al.[262] reported that some oxides directly produce ethyl acetate from ethanol. Acetaldehyde was formed by oxidative dehydrogenation and reacted further with the remaining alcohol to produce the ester. Bi₂O₃, MoO₃, and Sb₂O₄ showed good activity for ethyl acetate formation. However, binary oxides MoO₃–Sb₂O₄ showed much higher activity. Increased activity and increased selectivity for ethyl acetate were attributed to the formation Sb₄Mo₁₀O₃₁ during the course of the reaction. It is probable that these oxides in the aerogel form could still be much more effective and selective.

Bond and Flamerz[263] discussed the structure and reactivity of titania-supported oxides. Around 473 K, both titania (TiO₂) and vanadia (V₂O₅) act principally as dehydration catalysts. VOₓ/TiO₂ catalysts, prepared either by impregnation with NH₄VO₃–oxalic acid solutions or by grafting methods using VOCl₃ or VO(O-*i*-Bu)₃, exhibit a faster rate of acetone formation than propene formation. Rates were found to be almost independent of V₂O₅ content in the 1–10-monolayer range, and at the one-monolayer point were 50 times faster on a weight basis than with unsupported V₂O₅. Activation energies for both reactions—decomposition of 2-propanol (a) by dehydration to propene and (b) by dehydrogenation to acetone—are markedly lower for the monolayer catalysts than for the TiO₂ supports (with TiO₂ support, 147 kJ mol⁻¹; with 8% by weight V₂O₅–TiO₂, 17 kJ mol⁻¹), and selectivity to acetone increases with decreasing temperature. Activity is attributed to the vanadate groups in the monolayer, and a mechanism involving V=O and VOH groups is proposed for the dehydrogenation reaction.

ii. Aerogels for Gellifying Rocket Propellants

Because of the large pore volume of aerogels, a small weight of these solids may confine a large volume of liquid. Aerogels also appear to have the ability to develop viscosity and thixotropic behavior in liquids, and hence their use as good thickening agents for water, gasoline, red fuming nitric acid (RFNA), and unsymmetrical dimethylhydrazine (UMDH) in fuel. In all cases, the gels obtained are thixotropic viscoplastics with fairly high shear stress (e.g., 0.6 kPa) thresholds. The macropore volumes of aerogels govern their thickening capabilities. Teichner and co-workers[260b] were able to jellify more than 20 g of RFNA and 40 g of UMDH per 1 g of silica aerogel. The gellifying ability of aerogels is correlated with their macropore volume and is independent of their surface area.

iii. Aerogel Method for Carbon Composite Densification[260b]

Products deposited on a heated graphite substrate by vapor-phase pyrolytic decomposition of gaseous hydrocarbons are termed chemical vapor deposited pyrolytic carbon. Carbon composites are macroporous materials that must be filled by carbon black using thermal cracking of methane at high temperatures (CVPD process). They are used for rocket nozzles, oxidation-resisting units, molten-salt reactors, heat exchangers, etc. Standard CVPD conditions are 1000 °C and 1 kPa of methane. The CVPD process is time- and energy-consuming and does not lead to the maximum permissible density of the carbon composite. The same carbon composite can be impregnated by a solution of Si(OCH₃)₄ in methanol with the stoichiometric amount of water to yield a dense aerogel of 120 g/mL. This aerogel can then be evacuated in the autoclave under hypercritical conditions with respect to methanol, and the resulting composite containing silica aerogel is more easily amenable to densification by the CVPD process. In applying the silica aerogel method, one must ensure, however, minimum shrinkage and elimination of SiO₂. At 700 °C dense silica aerogels exhibit only slight shrinkage. Silica is finally vaporized at 2500 °C without damage to the carbon material.

iv. Silica Aerogels as Insecticides

It has been claimed that silica aerogel is a more efficient killer of wood termites than the well-known insecticide DDT.[257,264] Chemically inert dusts of very fine particle size and high surface area can kill insects in grain and seeds as well as other earthly anthropods such as mites, ticks, cockroaches, silverfish, ants, fleas, and termites by adsorbing and abrading their protective lipid layer. Mortality results from the rapid loss of body fluids from the organic tissue. This physical, rather than chemical, activity of aerogels as an insecticide would be a safe and desirable attribute from an environmental point of view.

Other applications of aerogels can be found in gel permeation chromatography, oil recovery, storage, and transportation of dangerous liquids.

VI. Conclusion

Aerogels are extremely porous, high-technology materials and show great promise in a variety of applications. The existence of a massive volume of literature concerned with the sol–gel process indicates the vast scope of the method. Widespread passive solar energy application of aerogels—primarily use as superinsulation—would require less expensive methods of production, especially in relation to drying. In order to be economically viable for large windows, the use of autoclaves must be avoided. An alternative freeze-drying method that employs solvents with higher melting points, developed in the authors' laboratory, appears to be a promising approach.

Addendum

The 2nd International Symposium on Aerogels was held in Montpellier, France, on Sept 21–23, 1988. The proceedings will be published.[266] The preparation and characterization of cryogels by the freeze-drying method were described in two papers by Pajonk.[266] Monolithic dry gels were not produced—only powders were obtained by this method. Further development work on the sol–gel synthesis of superconducting oxides has been reported.[267] The preparation and characterization of monolithic gels[268] and the effect of formamide on the sol–gel process have been extended to gel structure.[269] Reduced molybdenum oxides were produced by the sol–gel process.[270] The catalytic properties of such gels have yet to be examined. Another survey of the sol–gel process in chemical applications has been reported.[271]

VII. Acknowledgment

VIII. References

(1) (a) Cantin, M.; Casse, M.; Koch, L.; Jouan, R.; Mestreau, P.; Roussell, D.; Bonnin, F.; Moutel, J.; Teichner, S. J. *Nucl. Instrum. Methods* 1974, *118*, 177. (b) Cantin, M.; Casse, M.; Koch, L.; Jouan, R.; Mestreau, P.; Roussell, D.; Bonnin, F.; Moutel, J.; Teichner, S. J. *J. Chim. Phys.* 1974, *11–12*, 1537.
(2) Rubin, M.; Lampert, C. M. *Sol. Energy Mater.* 1983, *1*, 393.
(3) Fricke, J. *Sci. Am.* 1988, 92.
(4) Teichner, S. J.; Nicolaon, G. A.; Vicarini, M. A.; Gardes, G. E. E. *Adv. Colloid Interface Sci.* 1976, *5*, 245.
(5) Schmitt, W. J. "The Preparation and Properties of Acid Catalyzed Silica Aerogels", M.Sc. Thesis, University of Wisconsin, Madison, 1982.
(6) Livage, A.; Lemerle, J. *Annu. Rev. Mater. Sci.* 1982, *12*, 103.
(7) Fricke, J., Ed. *Aerogels* (Proceedings of the First International Symposium. Wurzburg, FRG, Sept 23–25, 1985); Springer-Verlag: Berlin, 1986.
(8) (a) Mahler, W.; Bechtold, M. F. *Nature (London)* 1980, *27*, 285. Nippon Telegraph and Telephone Public Corp. Jpn. Kokai Tokkyo Koho JP 81 1000 145 (Cl. C03B37/00), 1981; *Chem. Abstr.* 1982, *96*, 56751υ (Japanese Patent Tokkai 56-100145).
(9) (a) Pajonk, G. M, private communication. (b) Rabinovich, E. M.; Johnson, D. W., Jr.; MacChesney, J. B.; Vogel, E. M. *J. Am. Ceram. Soc.* 1983, *66*, 683. (c) Gesser, H. D.; Goswami, P. C., unpublished results.
(10) Kistler, S. S. *Nature (London)* 1931, *127*, 741; *J. Phys. Chem.* 1932, *36*, 52.
(11) (a) Kistler, S. S. U.S. Patent 2 093 454, 1937; *Chem. Abstr.* 1937, *31*, 8132⁷. (b) Kistler, S. S. U.S. Patent 2 188 007, 1940; *Chem. Abstr.* 1940, *34*, 3890.⁸
(12) Kistler, S. S. U.S. Patent 2 249 767, 1941; *Chem. Abstr.* 1941, *35*, 7076⁴.
(13) Peri, A. B. *J. Phys. Chem.* 1966, *70*, 2937.
(14) Nicolaon, G. "Contribution of l'etude des aerogels des silice", Ph.D. Thesis, University of Lyon, 1968.
(15) (a) Nicolaon, G. A.; Teichner, S. J. *Bull. Soc. Chim. Fr.* 1968, *5*, 1900. (b) Nicolaon, G. A.; Teichner, S. J. *Bull. Soc. Chim. Fr.* 1968, *5*, 1906. (c) Nicolaon, G. A.; Teichner, S. J. *Bull. Soc. Chim. Fr.* 1968, *8*, 3107. (d) Nicolaon, G. A.; Teichner, S. J. *Bull. Soc. Chim. Fr.* 1968, *9*, 3555. (e) Nicolaon, G. A.; Teichner, S. J. *Bull. Soc. Chim. Fr.* 1968, *11*, 4343. (f) Nicolaon, G. A.; Teichner, S. J. *J. Chim. Phys.* 1968, *65*, 1480.
(16) Teichner, S. J. U.S. Patent 3 672 833, 1972.
(17) Vicarini, M. A.; Nicalaon, G. A.; Teichner, S. J. *Bull. Soc. Chim. Fr.* 1970, *2*, 431.
(18) Moutel, J. "Preparation et etude des proprietes des aerogel de silice utilises comme radiateurs dans les detecteurs Cerenkov", Ph.D. Thesis, University of Claude Bernard, Lyon, 1977.
(19) Henning, S.; Svenson, L. *Phys. Scr.* 1981, *23*, 697.
(20) Poelz, G.; Riethmuller, R. "Preparation of silica aerogel for Cerenkov counters", Report 81-055, DESY (Deutches Electronen-Synchrotron), Sept 1981.
(21) Blanchard, F.; Pommier, B.; Reymond, J. P.; Teichner, S. J. In *Preparation of Catalysts III*; Poncelet, G., Grange, P., Jacobs, P. A., Eds.; Elsevier Science Publishers B.V.: Amsterdam, 1983; p 395.
(22) Sayari, A.; Ghorbel, A.; Pajonk, G. M.; Teichner, S. J. *Bull. Soc. Chim. Fr.* 1981, I-2, I-7, I-16.
(23) Schmidt, H.; Scholze, H., ref 7, p 49.
(24) Hubert-Pfalzgraf, L. G. *New J. Chem.* 1987, *11*, 663.
(25) Mehrotra, R. C. *J. Non-Cryst. Solids* 1988, *100*, 1.
(26) Guglielmi, M.; Carturan, G. *J. Non-Cryst. Solids* 1988, *100*, 16.
(27) Brinker, C. J. *J. Non-Cryst. Solids* 1988, *100*, 31.
(28) Linter, B.; Arfsten, N.; Dislich, H.; Schmidt, H.; Philipp, G.; Seiferling, B. *J. Non-Cryst. Solids* 1988, *100*, 378.
(29) Sanchez, C.; Livage, J.; Henry, M.; Babonneau, F. *J. Non-Cryst. Solids* 1988, *100*, 65.
(30) Schmidt, H. *J. Non-Cryst. Solids* 1988, *100*, 51.
(31) Kawai, H. *Nucl. Instrum. Methods Phys. Res.* 1985, *228*, 314.
(32) Emili, M. *J. Non-Cryst. Solids* 1985, *74*, 129.
(33) Sherer, C. P.; Pantano, C. G. *J. Non-Cryst. Solids* 1986, *82*, 246.
(34) Vance, E. R. *J. Mater. Sci.* 1986, *21*, 1413.
(35) Lirong, Y.; Guoxing, Y. *J. Non-Cryst. Solids* 1988, *100*, 309.
(36) Mukherjee, S. P.; Sharma, S. K. *J. Non-Cryst. Solids* 1985, *71*, 317.
(37) Shibata, S.; Kitagawa, T. *Jpn. J. Appl. Phys.* 1986, *25*, L323.
(38) Gimblett, F. G. R.; Rahman, A. A.; Sing, K. S. W. *J. Colloid Interface Sci.* 1981, *84*, 337.
(39) Veiga, M. L.; Vallet, M.; Jerez, A. *Ann. Chim. (Paris)* 1981, *6*, 341.
(40) Rahman, A. A.; Sing, K. S. W. *Thermochim. Acta* 1979, *29*, 277.
(41) Veiga Blanco, M. L.; Vallet Regi, M.; Mata Arjona, A.; Guttierez Rios, Y. E. *Ann. Quim.* 1980, *76B*, 346.
(42) Yamada, K.; Chow, T.; Horihata, T.; Nagata, M. *J. Non-Cryst. Solids* 1988, *100*, 316.
(43) Tohge, N.; Matsuda, A.; Minami, T. *Chem. Express* 1987, *2*, 141.
(44) Torralvo, M. J.; Alario, M. A. *J. Catal.* 1984, *86*, 473.
(45) Torralvo-Fernandez, M. J.; Alario-Franco, M. A. *J. Colloid Interface Sci.* 1980, *77*, 29.
(46) Yoko, T.; Yuasa, A.; Kamiya, K.; Tanaka, K.; Sakka, S. *J. Chem. Soc. Jpn., Chem. Ind. Chem.* 1987, *11*, 1951.
(47) Covina, J.; Nissan, R. A. *Mater. Res. Bull.* 1986, *21*, 337.

(48) Maki, T.; Sakka, S. *J. Non-Cryst. Solids* **1988**, *100*, 303.
(49) Tohge, N.; Matsuda, A.; Minami, T. *J. Chem. Soc. Jpn., Chem. Ind. Chem.* **1987**, *11*, 1957.
(50) Tatsumisaga, M.; Minami, T. *J. Chem. Soc. Jpn., Chem. Ind. Chem.* **1987**, *11*, 1963.
(51) Boilot, J. P. *Ann. Chim (Paris)* **1985**, *10*, 305.
(52) Desport, J. A.; Moseley, P. T.; Williams, D. E. *J. Mater. Sci. Lett.* **1982**, *1*, 288.
(53) Makashima, A.; Asami, M.; Wada, K. *J. Non-Cryst. Solids* **1988**, *100*, 321.
(54) Lemerle, J.; Nejem, L.; Lefebvre, J. *J. Chem. Res. (S)* **1978**, 444.
(55) Lemerle, J.; Nejem, L.; Lefebvre, J. *J. Chem. Res.* **1978**, 5301.
(56) (a) Lemerle, J.; Nejem, L.; Lefebvre, J. *J. Inorg. Nucl. Chem.* **1980**, *42*, 17. (b) Gharbi, N.; Sanchez, C.; Livage, J.; Lemerle, J.; Nejem, L.; Lefebvre, J. *Inorg. Chem.* **1982**, *21*, 2758.
(57) Aldebert, P.; Baffier, N.; Legendre, J. J.; Livage, J. *Rev. Chim. Miner.* **1982**, *19*, 485.
(58) Abello, L.; Husson, E.; Repelin, Y.; Lucazeau, G. *J. Solid State Chem.* **1985**, *56*, 379.
(59) Chemseddine, A.; Babonneau, F.; Livage, J. *J. Non-Cryst. Solids* **1987**, *91*, 287.
(60) Vaidya, V. N.; Mukerjee, S. K.; Joshi, J. K.; Kamat, R. V.; Sood, D. D. *J. Nucl. Mater.* **1987**, *148*, 324.
(61) Matthews, R. B.; Tewari, P. H.; Copps, T. P. *J. Colloid Interface Sci.* **1979**, *68*, 260.
(62) Fierro, J. L. G.; Mendoiroz, S.; Sanz, J. *J. Colloid Interface Sci.* **1983**, *93*, 487.
(63) Debsikdar, J. C. *J. Mater. Sci.* **1985**, *20*, 4454.
(64) Cocco, G.; Euzo, S.; Carturan, G.; Giordano Orsini, P.; Scardi, P. *Mater. Chem. Phys.* **1987**, *17*, 541.
(65) Russo, R. E.; Hunt, A. J. *J. Non-Cryst. Solids* **1986**, *86*, 219.
(66) Tewari, P. H.; Hunt, A. J.; Lofftus, K. D. *Mater. Lett.* **1985**, *3*, 363.
(67) Nguyen, D.; Gowda, G. *J. Can. Ceram. Soc.* **1985**, *54*, 40.
(68) Pezzo, T.; Botter, R.; Guglielmi, M.; Giordani, M.; Beruto, D. *Chim. Ind.* **1986**, *68*, 75.
(69) Avnir, D.; Kaufman, V. R. *J. Non-Cryst. Solids* **1987**, *192*, 180.
(70) Weres, O.; Yee, A.; Tsao, L. *J. Colloid Interface Sci.* **1981**, *84*, 379.
(71) Klein, L. C.; Garvey, G. J. *J. Non-Cryst. Solids* **1980**, *38–39*, 45.
(72) Klein, L. C.; Garvey, G. J. *J. Non-Cryst. Solids* **1982**, *48*, 97.
(73) (a) Abe, Y.; Misono, T. *J. Polym. Sci., Polym. Lett.* **1982**, *20*, 205. (b) Abe, Y.; Sekiguchi, T.; Misono, T. *J. Polym. Sci., Polym. Chem. Ed.* **1984**, *22*, 761.
(74) Abe, Y.; Misono, T. *J. Polym. Sci., Polym. Lett.* **1984**, *22*, 565.
(75) Bechtold, M. F.; Mahler, W.; Schunn, R. A. *J. Polym. Sci., Polym. Chem. Ed.* **1980**, *18*, 2828.
(76) Mizuno, T.; Phalippou, J.; Zarzycki, J. *Glass Technol.* **1985**, *26*, 39.
(77) (a) Pope, E. J. A.; Mackenzie, J. D. *J. Non-Cryst. Solids* **1988**, *101*, 198. (b) Colby, M. W.; Osaka, A.; Mackenzie, J. D. *J. Non-Cryst. Solids* **1988**, *99*, 129.
(78) Hoffman, D. W.; Roy, R.; Komarneni, S. *J. Am. Ceram. Soc.* **1984**, *67*, 468.
(79) Hoffman, D.; Komarneni, S.; Roy, R. *J. Mater. Sci. Lett.* **1984**, *3*, 439.
(80) Roy, R. A.; Roy, R. *Mater. Res. Bull.* **1984**, *19*, 1969.
(81) Hoffman, D.; Roy, R.; Komarneni, S. *Mater. Lett.* **1984**, *2*, 245.
(82) Arend, H.; Connelly, J. J. *J. Cryst. Growth* **1982**, *56*, 642.
(83) Komarneni, S.; Breval, E.; Roy, R. *J. Non-Cryst. Solids* **1986**, *79*, 195.
(84) Kokubu, T.; Yamane, M. *J. Mater. Sci.* **1987**, *22*, 2583.
(85) (a) Tewari, P. H.; Hunt, A. J.; Lofftus, K. D., ref 7, p 31. (b) Tewari, P. H.; Hunt, A. J. "Forming Transparent Aerogel Insulating Arrays", U.S. Patent 4610863, 1986; *Chem. Abstr.* **1986**, *105*, 214727c.
(86) Zarzycki, J.; Woignier, T., ref 7, p 42.
(87) Brinker, C. J.; Ward, K. J.; Keefer, K. D.; Holupka, E.; Bray, P. J.; Pearson, R. K., ref 7, p 57.
(88) Little, L. H., private communication.
(89) Yoldas, B. E. *Am. Ceram. Soc. Bull.* **1975**, *54*, 286.
(90) Yoldas, B. E. *J. Mater. Sci.* **1975**, *10*, 1856.
(91) Yoldas, B. E. *J. Non-Cryst. Solids* **1980**, *38–39*, 81.
(92) Yoldas, B. E. *Am. Ceram. Soc. Bull.* **1975**, *54*, 289.
(93) (a) Yoldas, B. E. "Transparent Activated Non-Particulate Alumina and Method of Preparing Same", U.S. Patent 3941719, 1976; *Chem. Abstr.* **1976**, *84*, 166860q. (b) Yoldas, B. E. "Transparent Activated Non-Particulate Alumina and Method of Preparing Same", U.S. Patent 3944658, 1976; *Chem. Abstr.* **1976**, *84*, 182148u.
(94) Mazur, J. H.; Lampert, C. M. "High-Resolution Electron Microscopy", 28th SPIE Annual International Technical Symposium, San Diego, CA, Aug 19–24, 1984.
(95) Dumas, J., et al. *J. Mater. Sci. Lett.* **1985**, *4*, 1089.
(96) Tewari, P. H.; Hunt, A. J.; Lieber, J. G., ref 7, p 142.
(97) Schuck, G.; Dietrich, W., ref 7, p 148.

(98) Lampert, C. M.; Mazur, J. H., ref 7, p 154.
(99) Broecker, F. J.; Heckmann, W.; Fischer, F.; Mielke, M.; Schroeder, J.; Stange, A., ref 7, p 160.
(100) (a) Gronauer, M.; Kadur, A.; Fricke, J., ref 7, p 167. (b) Courtens, E.; Pelous, J.; Phalippou, J.; Vacher, R.; Woignier, T. *J. Non-Cryst. Solids* **1987**, *95–96*, 1175. (c) Woignier, T.; Phalippou, J. *J. Non-Cryst. Solids* **1988**, *100*, 404. (d) Woignier, T.; Phalippou, J.; Sempere, R.; Pelous, J. *J. Phys. (Paris)* **1988**, *49*, 289. (e) Woignier, T.; Pelous, J.; Phalippou, J.; Vacher, R.; Courtens, E. *J. Non-Cryst. Solids* **1987**, *95–96*, 1197.
(101) Fricke, J.; Reichenauer, G. *J. Non-Cryst. Solids* **1987**, *95–96*, 1135.
(102) Woignier, T.; Phalippou, J. *J. Non-Cryst. Solids* **1987**, *93*, 17.
(103) da Silva, A. A.; dos Santos, D. I.; Aegerter, M. A. *J. Non-Cryst. Solids* **1987**, *95–96*, 1159.
(104) (a) Courtens, E.; Pelous, J.; Phalippou, J.; Vacher, R.; Woignier, T. *Phys. Rev. Lett.* **1987**, *58*, 128. (b) Vacher, R.; Woignier, T.; Pelous, J. *Phys. Rev. B.* **1988**, *37*, 65.
(105) dos Santos, D. I.; Aegerter, M. A. *J. Non-Cryst. Solids* **1987**, *95–96*, 1143.
(106) Boukenier, A.; Champagnon, B.; Dumas, J.; Duval, E.; Quinson, J. F.; Serughetti, J. *J. Non-Cryst. Solids* **1987**, *95–96*, 1189.
(107) Wood, D. L.; Rabinovich, E. M. *J. Non-Cryst. Solids* **1986**, *82*, 171.
(108) Quinson, J. F.; Dumas, J.; Serughetti, J. *J. Non-Cryst. Solids* **1986**, *79*, 397.
(109) Dumas, J.; Baza, S.; Serughetti, J. *J. Mater. Sci. Lett.* **1986**, *5*, 478.
(110) Rosenberger, H.; Scheler, G.; Burger, H.; Jakob, M. *Colloids Surf.* **1984**, *12*, 52.
(111) Sindorf, D. W.; Maciel, G. E. *J. Phys. Chem.* **1983**, *87*, 5516.
(112) Kelts, L. W.; Effinger, N. J.; Mellpolder, S. M. *J. Non-Cryst. Solids* **1986**, *83*, 353.
(113) Kordas, G.; Weeks, R. A.; Klein, L. C. *J. Non-Cryst. Solids* **1985**, *71*, 327.
(114) Klein, L. C.; Kordas, G. *Mater. Res. Soc. Symp. Proc.* **1986**, *73*, 461.
(115) Wolf, A. A.; Friebele, E. J.; Tran, D. C. *J. Non-Cryst. Solids* **1985**, *71*, 345.
(116) Artaki, I.; Bradley, M.; Zerda, T. W.; Jonas, J. *J. Phys. Chem.* **1985**, *89*, 4399.
(117) Orcel, G.; Hench, L. *J. Non-Cryst. Solids* **1986**, *79*, 177.
(118) Rosenberger, H.; Burger, H.; Schutz, H.; Scheler, G.; Maenz, G. *Z. Phys. Chem. (Frankfurt/Main)* **1987**, *153*, 5, 27.
(119) Adachi, T.; Sakka, S. *J. Non-Cryst. Solids* **1988**, *100*, 250.
(120) (a) Mizuno, T.; Nagata, H.; Manabe, S. *J. Non-Cryst. Solids* **1988**, *100*, 236. (b) Kozuka, H.; Kuroki, H.; Sakka, S. *J. Non-Cryst. Solids* **1987**, *95–96*, 1181.
(121) Anderson, P.; Klein, L. C. *J. Non-Cryst. Solids* **1987**, *93*, 415.
(122) Yoldas, B. *J. Non-Cryst. Solids* **1986**, *82*, 11.
(123) Yoldas, B. *J. Non-Cryst. Solids* **1986**, *83*, 375.
(124) Sakka, S.; Tanaka, Y.; Kokubo, T. *J. Non-Cryst. Solids* **1986**, *82*, 24.
(125) Lasic, D. D. *J. Colloid Interface Sci.* **1986**, *110*, 282.
(126) Chen, K. C.; Tsuchiya, T.; Mackenzie, J. D. *J. Non-Cryst. Solids* **1986**, *81*, 227.
(127) Orgaz, F.; Rawson, H. *J. Non-Cryst. Solids* **1986**, *82*, 57, 378.
(128) Weatherwax, R. C. *J. Colloid Interface Sci.* **1977**, *62*, 432.
(129) Tanioka, A., et al. *J. Appl. Polym. Sci.* **1984**, *29*, 583.
(130) Scherer, G. W., private communication.
(131) Poelz, G., ref 7, p 176.
(132) Koch-Miramond, L., ref 7, p 188.
(133) Zarzycki, J. W.; Prassas, M.; Phalippou, J. E. H. "Aerogels de silice monolithiques leur preparation et leur utilization pour la preparation d'articles en verre de silice et de materiaux thermiquement isolants", French Patent 2507171, 1982.
(134) Hunt, A. J. "Microporous Transparent Materials for Insulating Windows and Building Applications", Lawrence Berkeley Laboratory, University of California, Assessment Report, 15306, UC-95d, Nov 1982.
(135) Hunt, A. J. "Light Scattering Studies of Silica Aerogels", Lawrence Berkeley Laboratory, University of California, Report 15756, Feb 1983.
(136) Schmitt, W. J.; Greiger-Block, R. A.; Chapman, T. W. "The Preparation of Acid Catalyzed Silica Aerogels". Presented at the annual meeting of the AICHE, New Orleans, 1981.
(137) Kistler, S. S. *J. Phys. Chem.* **1935**, *39*, 79.
(138) Kistler, S. S. *J. Phys. Chem.* **1942**, *46*, 19.
(139) Kistler, S. S.; Caldwell, A. G. *Ind. Eng. Chem.* **1934**, *26*, 658.
(140) Fricke, J. *J. Non-Cryst. Solids* **1988**, *100*, 169.
(141) Caps, R.; Fricke, J. *Sol. Energy* **1986**, *36*, 361.
(142) Hartmann, J.; Rubin, M.; Arasteh, D. "Thermal and Solar-Optical Properties of Silica Aerogel for use in Insulated Windows". *Solar '87, 12th Passive Solar Conference Proceedings, July 11–16, 1987, Portland, Oregon*; Andrejko, D., Hayes, J., Eds.; The American Solar Energy Society Inc. and the Solar Energy Society of Canada Inc.: **1987**, 42.
(143) Goetzberger, A.; Wittwer, V., ref 7, p 84.

(144) Fricke, J.; Caps, R.; Buttner, D.; Heinemann, U.; Hummer, E. *Sol. Energy Mater.* **1987**, *16*, 267.
(145) Nilsson, O.; Fransson, A.; Sandberg, O., ref 7, p 121.
(146) Platzer, W.; Wittwer, V.; Mielke, M., ref 7, p 127.
(147) Schreiber, E.; Boy, E.; Bertsch, K., ref 7, p 133.
(148) Berman, E.; Wildes, P. In *Luminescent Solar Concentrators. Photochemical Conversion and Storage of Solar Energy. Part A (4th International Conference)*; Rabani, J., Ed.; Weizmann Science Press of Israel: Jerusalem, 1982; p 43.
(149) Reisfeld, R.; Jorgensen, C. K. In *Struct. Bonding (Berlin)* **1982**, *49*, 1.
(150) Reisfeld, R. *J. Electrochem. Soc.* **1984**, *131*, 1364.
(151) Folcher, G.; Keller, N.; Paris, J. *Sol. Energy Mater.* **1984**, *10*, 303.
(152) Avnir, D.; Levy, D.; Reisfeld, R. *J. Phys. Chem.* **1984**, *88*, 5956.
(153) Dechottignies, M., et al. *J. Mater. Sci.* **1978**, *13*, 2605.
(154) Iino, A.; Mizuike, A. *Bull. Chem. Soc. Jpn.* **1979**, *52*, 2433.
(155) Puyane, R.; James, P. F.; Rawson, H. *J. Non-Cryst. Solids* **1980**, *41*, 105.
(156) Hayashi, T.; Saito, H. *J. Mater. Sci.* **1980**, *15*, 1971.
(157) Brinker, C. J.; Mukherjee, S. P. *J. Mater. Sci.* **1980**, *16*, 1980.
(158) Mukherjee, S. P. *J. Non-Cryst. Solids* **1980**, *42*, 477.
(159) Sakka, S.; Kamiya, K. *J. Non-Cryst. Solids* **1980**, *42*, 403.
(160) Nogami, M.; Moriya, Y. *J. Non-Cryst. Solids* **1980**, *37*, 191.
(161) (a) Yoldas, B. E. *J. Non.-Cryst. Solids* **1980**, *38–39*, 81. (b) Yoldas, B. C. *J. Mater. Sci.* **1976**, *11*, 456. (c) Yoldas, B. E. *J. Mater. Sci.* **1976**, *11*, 456. (d) Yoldas, B. E. *J. Mater. Sci.* **1979**, *14*, 1843.
(162) Gorlich, E. *Ann. Chim. (Paris)* **1980**, *5*, 597.
(163) Yamane, M.; Kojima, T. *J. Non-Cryst. Solids* **1981**, *44*, 181.
(164) Kamiya, K.; Sakka, S. *J. Chem. Soc. Jpn., Chem. Ind. Chem.* **1981**, 1571.
(165) Nogmai, G.; Moriya, Y. *J. Non-Cryst. Solids* **1982**, *48*, 359.
(166) (a) Yoldas, B. E. *J. Mater. Sci.* **1976**, *118*, 456. (b) Yoldas, B. E. *J. Mater. Sci.* **1977**, *12*, 1203. (c) Yoldas, B. E. *J. Mater. Sci.* **1979**, *14*, 1843.
(167) (a) Reference 9b. (b) Johnson, D. W., Jr.; Rabinovich, E. M.; MacChesney, J. B.; Vogel, E. M. *J. Am. Ceram. Soc.* **1983**, *66*, 688. (c) Wood, D. W.; Rabinovich, E. M.; Johnson, D. W., Jr.; MacChesney, J. B.; Vogel, E. M. *J. Am. Ceram. Soc.* **1983**, *66*, 693.
(168) Schmidt, H.; Scholze, H.; Kaiser, A. *J. Non-Cryst. Solids* **1984**, *63*, 1.
(169) Yamane, M.; Inoue, S.; Yasumori, A. *J. Non-Cryst. Solids* **1984**, *63*, 13.
(170) Klein, L. C.; Gallo, T. A.; Garvey, G. J. *J. Non-Cryst. Solids* **1984**, *63*, 23.
(171) Mukherjee, S. P. *J. Non-Cryst. Solids* **1984**, *63*, 35.
(172) Brinker, C. J.; Keefer, K. D.; Schaefer, D. W.; Assink, R. A.; Kay, B. D.; Ashley, C. S. *J. Non-Cryst. Solids* **1984**, *63*, 45.
(173) Kawaguchi, T.; Hishikura, H.; Iura, J.; Kokubu, Y. *J. Non-Cryst. Solids* **1984**, *63*, 61.
(174) Gottardi, V.; Guglielmi, M.; Bertoluzza, A.; Fagnano, C.; Morelli, M. S. *J. Non-Cryst. Solids* **1984**, *63*, 71.
(175) Pancrazi, F.; Phalippou, J.; Sorrentino, F.; Zarzycki, J. *J. Non-Cryst. Solids* **1984**, *63*, 81.
(176) Tohge, N.; Moore, G. S.; Mackenzie, J. D. *J. Non-Cryst. Solids* **1984**, *63*, 95.
(177) Congshen, Z.; Lisong, H.; Fuxi, G.; Zhonghong, J. *J. Non-Cryst. Solids* **1984**, *63*, 105.
(178) Woignier, T.; Phalippou, J.; Zarzycki, J. *J. Non-Cryst. Solids* **1984**, *63*, 117.
(179) Krol, D. M.; Van Lierop, J. G. *J. Non-Cryst. Solids* **1984**, *63*, 131.
(180) Yoldas, B. E. *J. Non-Cryst. Solids* **1984**, *63*, 145.
(181) Rabinovich, E. M.; MacChesney, J. B.; Johnson, D. W., Jr.; Simpson, J. R.; Meagher, B. W.; DiMarcello, F. V.; Wood, D. L.; Sigety, E. A. *J. Non-Cryst. Solids* **1984**, *63*, 155.
(182) Scherer, C. W.; Luong, J. C. *J. Non-Cryst. Solids* **1984**, *63*, 163.
(183) Schlichting, J. *J. Non-Cryst. Solids* **1984**, *63*, 173.
(184) Segal, D. L. *J. Non-Cryst. Solids* **1984**, *63*, 183.
(185) Pentinghaus, H. *J. Non-Cryst. Solids* **1984**, *63*, 193.
(186) Jones, K.; Emblem, H. G.; Hafez, H. M. *J. Non-Cryst. Solids* **1984**, *63*, 201.
(187) Glaser, P. M.; Pantano, C. G. *J. Non-Cryst. Solids* **1984**, *63*, 209.
(188) Sakka, S.; Kamiya, K.; Makita, K.; Yamamoto, Y. *J. Non-Cryst. Solids* **1984**, *63*, 223.
(189) Dislich, H. *J. Non-Cryst. Solids* **1984**, *63*, 237.
(190) Arfsten, N. *J. Non-Cryst. Solids* **1984**, *63*, 243.
(191) Geotti-Bianchini, F.; Guglielmi, M.; Polato, P.; Soraru, G. D. *J. Non-Cryst. Solids* **1984**, *63*, 251.
(192) Kaiser, A.; Schmidt, H. *J. Non-Cryst. Solids* **1984**, *63*, 261.
(193) Carturan, G.; Facchin, G.; Gottardi, V.; Navazio, G. *J. Non-Cryst. Solids* **1984**, *63*, 273.
(194) Philipp, G.; Schmidt, H. *J. Non-Cryst. Solids* **1984**, *63*, 283.
(195) Mulder, C. A. M.; Van Lierop, J. G., ref 7, p 68.
(196) Achtsnit, H. D., ref 7, p 76.

(197) Pettit, R. B.; Brinker, C. J. *Sol. Energy Mater.* **1986**, *14*, 269.
(198) Avnir, D.; Kaufman, V. R.; Reisfeld, R. *J. Non-Cryst. Solids* **1985**, *74*, 395.
(199) Partlow, D. P.; Yoldas, B. E. *J. Non-Cryst. Solids* **1981**, *46*, 153.
(200) Bertoluzza, A.; Fagnano, C.; Gottardi, V.; Guglielmi, M. *J. Non-Cryst. Solids* **1982**, *48*, 117.
(201) Yamane, M.; Inoue, S.; Nakazawa, K. *J. Non-Cryst. Solids* **1982**, *48*, 153.
(202) Gonzalez-Oliver, C. J. R.; James, P. F.; Rawson, H. *J. Non-Cryst. Solids* **1982**, *48*, 129.
(203) Hayashi, T.; Yamada, T.; Saito, H. *J. Mater. Sci.* **1983**, *18*, 3137.
(204) Hoffman, D. W.; Roy, R.; Komarneni, S. *J. Am. Ceram. Soc.* **1984**, *67*, 468.
(205) Tohge, N.; Mackenzie, J. D. *J. Non-Cryst. Solids* **1984**, *68*, 411.
(206) Dislich, H. *J. Non-Cryst. Solids* **1983**, *57*, 371.
(207) Ehrburger, F.; Guerin, V.; Lahaye, J. *Colloids Surf.* **1984**, *9*, 371.
(208) Ehrburger, F.; Guerin, V.; Lahaye, J. *Colloids Surf.* **1985**, *14*, 31.
(209) Wills, R. R.; Markle, R. A.; Mukherjee, S. P. *Am. Ceram. Soc. Bull.* **1983**, *62*, 904.
(210) Zarzycki, J. *J. Non-Cryst. Solids* **1982**, *48*, 105.
(211) Best, M. F.; Dondrate, R. A., Sr. *J. Mater. Sci. Lett.* **1985**, *4*, 994.
(212) Wenzel, J. *J. Non-Cryst. Solids* **1985**, *73*, 693.
(213) Wenzel, J. "*Glass: Current Issues*"; Wright, A., Dupuy, J., Eds.; Nijhoff: Dordrecht, 1985; p 224.
(214) Bonner, F. J.; Kordas, G.; Kinser, D. L. *J. Non-Cryst. Solids* **1985**, *71*, 361.
(215) Brinker, C. J.; Scherer, G. W. *J. Non-Cryst. Solids* **1985**, *70*, 301.
(216) Brinker, C. J.; Scherer, G. W.; Roth, E. P. *J. Non-Cryst. Solids* **1985**, *72*, 345.
(217) Scherer, G. W.; Brinker, C. J.; Roth, E. P. *J. Non-Cryst. Solids* **1985**, *72*, 369.
(218) Brinker, C. J.; Roth, E. P.; Scherer, G. W.; Tallant, D. R. *J. Non-Cryst. Solids* **1985**, *71*, 171.
(219) Gottardi, V. *J. Non-Cryst. Solids* **1985**, *73*, 625.
(220) Orgaz, F.; Rawson, H. *J. Non-Cryst. Solids* **1986**, *82*, 378.
(221) Gonzalez-Oliver, C. J. R.; Kato, I. *J. Non-Cryst. Solids* **1986**, *82*, 400.
(222) Mulder, C. A. M.; van Lierop, J. G.; Frens, G. *J. Non-Cryst. Solids* **1986**, *82*, 92.
(223) Nassaau, K.; Rabinovich, E. M.; Miller, A. E.; Gallagher, P. K. *J. Non-Cryst. Solids* **1986**, *82*, 78.
(224) van Lierop, J. G.; Hunizing, A.; Meerman, W. C. P. M.; Mulder, C. A. *J. Non-Cryst. Solids* **1986**, *82*, 265.
(225) Scherer, G. W. *J. Non-Cryst. Solids* **1986**, *87*, 199.
(226) Scherer, G. W. *J. Non-Cryst. Solids* **1987**, *89*, 217.
(227) Scherer, G. W. *J. Non-Cryst. Solids* **1987**, *91*, 83.
(228) Scherer, G. W. *J. Non-Cryst. Solids* **1987**, *91*, 101.
(229) Scherer, G. W. *J. Non-Cryst. Solids* **1987**, *92*, 122.
(230) Scherer, G. W. *J. Non-Cryst. Solids* **1987**, *92*, 375.
(231) Scherer, G. W. *J. Non-Cryst. Solids* **1988**, *100*, 77.
(232) Scherer, G. W. *Surf. Colloid Sci.* **1987**, *14*, 264.
(233) Mackenzie, J. D. *J. Non-Cryst. Solids* **1988**, *100*, 162.
(234) Quinson, J. F.; Tchipkam, N.; Dumas, J.; Bovier, C.; Seru-ghetti, J. *J. Non-Cryst. Solids* **1988**, *100*, 231.
(235) Dislich, H. *J. Non-Cryst. Solids* **1986**, *80*, 115.
(236) Duran, A. *J. Non-Cryst. Solids* **1988**, *82*, 69.
(237) Schmidt, H.; Scholze, H.; Gunker, G. *J. Non-Cryst. Solids* **1986**, *80*, 557.
(238) Kordas, G.; Klein, L. C. *J. Non-Cryst. Solids* **1986**, *84*, 325.
(239) Kawaguchi, T. *J. Non-Cryst. Solids* **1986**, *82*, 50.
(240) Strawbridge, I.; James, P. F. *J. Non-Cryst. Solids* **1986**, *86*, 381.
(241) Sakka, S. *J. Non-Cryst. Solids* **1985**, *73*, 651.
(242) Neilson, G. F.; Weinberg, M. C. *J. Non-Cryst. Solids* **1984**, *63*, 365.
(243) Ulrich, D. R. *J. Non-Cryst. Solids* **1988**, *100*, 174.
(244) Krol, D. M.; Mulder, C. A. M.; van Lierop, J. G. *J. Non-Cryst. Solids* **1986**, *86*, 241.
(245) Suwa, Y.; Roy, R.; Komarneni, S. *Mater. Sci. Eng.* **1986**, *83*, 151.
(246) Oda, K.; Yoshio, T. *J. Mater. Sci. Lett.* **1986**, *5*, 545.
(247) Sun, K.; Lee, W. H.; Risen, W. M., Jr. *J. Non-Cryst. Solids* **1987**, *92*, 145.
(248) Tanaka, T.; Sun, S. T.; Hirokawa, Y.; Katayama, S.; Kucera, J.; Hirose, Y.; Amiya, T. *Nature (London)* **1987**, *325*, 796.
(249) Barboux, P.; Gourier, D.; Livage, J. *Colloids Surf.* **1984**, *11*, 119.
(250) Bali, K.; Kiss, L. B.; Szorenyi, T.; Torok, M. I.; Hevesi, I. *J. Phys. (Paris)* **1987**, *48*, 431.
(251) Calemczuk, R.; DeGoer, A. M.; Salce, B.; Maynard, R.; Za-rembowitch, A. *Europhys. Lett.* **1987**, *3*, 1205.
(252) Woodhead, J. L.; Segal, D. L. *Chem. Br.* **1984**, *20*, 310.
(253) Plodinec, M. J. *J. Non-Cryst. Solids* **1986**, *84*, 206.

(254) Yoko, T.; Kamiya, K.; Sakka, S. *Denki Kagaku* **1986**, *54*, 284.
(255) Yoko, T.; Kamiya, K.; Yuasa, A. *J. Electroanal. Chem.* **1986**, *209*, 399.
(256) (a) Roy, R. *Science* **1987**, *238*, 1664. (b) Kordas, G.; Wu, K.; Brahme, U. S.; Friedmann, T. A.; Ginsberg, D. M. *Mater. Lett.* **1987**, *5*, 417. (c) Monde, T.; Kozuka, H.; Sakka, S. *Chem. Lett.* **1988**, 290.
(257) Teichner, S. J., ref 7, p 22.
(258) Gesser, H. D.; Kruczynski, L. *J. Phys. Chem.* **1984**, *88*, 2751.
(259) Ragai, J. *Nature (London)* **1987**, *325*, 703.
(260) (a) Blanchard, F.; Reymond, J. P.; Pommier, B.; Teichner, S. J. *J. Mol. Catal.* **1982**, *17*, 171. (b) Pajonk, G. M.; Teichner, S. J., ref 7, p 193.
(261) (a) Armor, J. N.; Carlson, E. J.; Zambri, P. M. *Appl. Catal.* **1985**, *19*, 339. (b) Armor, J. N.; Carlson, E. J. *Appl. Catal.* **1985**, *19*, 327.

(262) Wang, L.; Eguchi, K.; Arai, H.; Seiyama, T. *Appl. Catal.* **1987**, *33*, 107.
(263) Bond, G. C.; Flamerz, S. *Appl. Catal.* **1987**, *33*, 219.
(264) Sen-Sarma, P. K.; Mishra, S. C. *Indian J. Entomol.* **1976**, *38*, 77.
(265) Perry, R. H.; Chilton, C. H. *Chemical Engineers' Handbook*, 5th ed.; McGraw-Hill: New York, 1973; pp 11–51.
(266) Proceedings of the 2nd International Symposium on Aerogels, Les Éditions de Physique (Paris), 1989.
(267) Ravindranathan, P.; Komarneni, S.; Bhalla, A.; Rag, A.; Cross, I. E. *J. Mater. Res.* **1988**, *3*, 810.
(268) Sivade, A., et al. *J. Non-Cryst. Solids* **1988**, *105*, 232.
(269) Orcel, G., et al. *J. Non-Cryst. Solids* **1988**, *105*, 223.
(270) Nogano, M.; Greenblatt, M. *J. Non-Cryst. Solids* **1988**, *101*, 255.
(271) Schmidt, H. *J. Non-Cryst. Solids* **1988**, *100*, 51.